International Journal of Advanced Manufacturing Technology

In-situ Quality Control of the Selective Laser Melting Process using a High Speed, Real-Time Melt Pool Monitoring System

--Manuscript Draft--

Manuscript Number:	JAMT-D-14-00830R1
Full Title:	In-situ Quality Control of the Selective Laser Melting Process using a High Speed, Real-Time Melt Pool Monitoring System
Article Type:	Original Research
Keywords:	Process monitoring; Selective Laser Melting; FPGA; High Speed; Real-Time
Corresponding Author:	Stijn Clijsters KU Leuven Heverlee, BELGIUM
Corresponding Author Secondary Information:	
Corresponding Author's Institution:	KU Leuven
Corresponding Author's Secondary Institution:	
First Author:	Stijn Clijsters
First Author Secondary Information:	
Order of Authors:	Stijn Clijsters
	Tom Craeghs, Dr. Ir.
	Sam Buls, M.Sc
	Karolien Kempen, M.Sc.
	Jean-Pierre Kruth, Prof. Dr. Ir.
Order of Authors Secondary Information:	
Abstract:	This paper discusses the principle and the relevance of an in-situ monitoring system for Selective Laser Melting (SLM). This system enables the operator to monitor the quality of the SLM job on-line and estimate the quality of the part accordingly. The monitoring system consists of two major developments in hardware and software. The first development, essential for a suitable monitoring system, is the design of a complete optical sensor set-up. This set-up is equipped with two commercially available optical sensors connected to a FPGA which communicates directly with the machine control unit. While the sensors ensure a high quality measurement of the melt pool, the FPGA's main task is to transfer the images from the sensors into relevant values at high sample rates (above 10kHz). The second development is the data analysis system to translate and visualize measured sensor values in the format of interpretable process quality images. The visualization is mainly done by a 'Mapping algorithm', which transfers the measurements from a time-domain into a position-domain representation. Further off-line experiments illustrate an excellent compatibility between the in-situ monitoring and the actual quality of the products. The resulting images coming out of this model, illustrate melt pool variations which can be linked to pores that are present in the parts.

RESPONSE TO REVIEWER COMMENTS:

Reviewer #1: This paper discuss an in-situ quality monitoring of Selective Laser Melting (SLM) process. The authors used optical sensors and a FPGA-based mapping system to analyze and visualize the collected data. The paper is very well written. But it comes short. The authors should consider following before the paper could be accepted.

- Mapping of XY- and XZ-planes shown in Figure 11-12(a) don't correctly represent the actual microscopic images shown in Figure 11-12(b). The authors need to explain the reasons for these variations and how this could influence the results.

- The authors used only one example made with NiTinol to validate their results. The analysis and validation should be made with more examples and also with different materials. This critical to prove that the developed method can be used robustly for any parts.

This is very well written paper and address an important problem for measuring and controlling in-situ quality of SLM parts. However, the paper comes short in getting empirical results and tuning-in the corresponding benchmark data for various materials and scans. This paper would enhance a lot and will have a big impact if those analyses are complete.

Dear Reviewer 1: Thank you for your constructive comments, your comments helped me to further improve the paper. I have taken them in consideration and have added the following things:

Considering the figures (11 and 12): I have added:
However it is important to notice that pores in the microscopic image are not located on the same locations as on the mappings. The mismatch between the similar X,Z- or X,Y-planes for mapping and microscopic images is due to the polishing of the specimen. Polishing exactly in a known plane is impossible. Both images show similar trends vertical pores in the X,Z-plane and a pore pattern in the X,Y-plane and are expected to match. To validate this some further tests have been conducted to validate the mappings with Computed Tomography.

Considering the remark on a lack of empirical data different materials, I have added another validation example of AlSi10Mg. In this example pores can be correlated to the mappings showing that the system has a lot of potential.

Reviewer #2: The paper is about in-situ quality control of an additive manufacturing process, SLM. The work includes valuable contributions to the field. In fact, there are some works with similar content and all are aiming in-situ quality control in SLM. In order to increase the robustness of the paper value, the related literature should be discussed well and the gaps in the literature should be highlighted clearly. Thus, the authors should elaborate the literature discussion part in introduction section.

The abstract of the paper should also be revised by giving the results of developed and/or introduced quality control system. Contributions of the work to the field should also be highlighted. The last sentence starting with, 'In the near future….' Should be removed from the abstract.

Dear Reviewer 2: Thank you for your relevant comments; they have improved the structure and value of my paper. Below I have listed the changes I have done based on your remarks:

I have modified the abstract by deleting the ‘in the near future…’ sentence and by adding the results of the system.

I also moved the literature part up to the introduction and extended a little bit. Besides this I added:

All these systems show a lot of similarities, for instance the coaxial set-up, however most systems do not sample signals at high rates and/or interpret them immediately (in Real-Time). These things are necessary to implement Real-Time feedback control.

Besides the Real-Time, the measured signals in all the systems found in literature are measured and visualized in time. This makes the interpretation of these sensor values difficult. Therefore in current developed system the position is sampled together with the melt pool sensor values, to open up new possibilities of data visualization and interpretation.

Reviewer #4: It shows an interesting development. But as you say: The monitoring system consists of two major developments in hardware and software. Unfortunately, the software part doesn't show in the text. Please also claim strongly about your contribution in both qualitative and quantitative viewpoints.

Dear reviewer 4 thank you for your constructive comments. I have taken your remarks in consideration and have therefore added some references to the software part such as:

The following sections on Reference Data and Estimating the quality are all implemented in software components. This implementation is besides the hardware development a new method of analyzing and visualizing the data, to predict the quality of parts.

To claim strongly about the contribution I added a small paragraph on the resolutions and accuracy

The resolution and accuracy of this quality control system is determined by the mapping algorithm and the sample rate. Currently each pixel of a mapped image is 100µm by 100µm The pixel size is selected based on the expected melt pool size (around 120-150µm diameter) and sample rate. Therefore a pixel where the melt pool is mapped will definitely be influenced by the measured melt pool signal. The automatic detection of very small pores (smaller than 100µm) will need, due to the big pixel size, a more complex algorithm than just tresholding.

Cover Letter - In-situ Quality Control of the Selective Laser Melting Process using a High Speed, Real-Time Melt Pool Monitoring System

S.Clijsters · T. Craeghs · S. Buls · K. Kempen · J.-P. Kruth

What is your main contribution to the field?

- The already existing monitoring system is upgraded to sample extra information that is crucial to understand the process better.
    - Position
    - Type of vector
- By adding Field Programmable Gate Arrays to the monitoring setup measurements of the melt pool at high sample rates of 20kHz can be done. These measurements open up possibilities (due to the extra data of position and vector type):
    - Better understanding of the process (illustrated in the paper)
    - Allows estimating the quality of a produced part (illustrated in the paper) based on a statistical method and an easy to understand representation based on the position of the sample.
    - Allows the possibility for future Feedback

What is Novel? In theory, in experimental techniques, or a combination of both?

- The implementation of FPGA's for image processing in the field of Additive Manufacturing is novel.
- The statistical analysis of the melt pool data is developed to have a robust method to estimate the quality of a part.
- The interpretation method of the data is novel.

Does your paper have industrial applications? If yes, who are the likely user?

This research in this paper has been conducted in close cooperation with a Laser beam melting machine vendor. They have great interest in this topic and are planning to create a similar implementation on their systems.

On conferences lot of research institutes showed their interest in this developed system.

International Journal of Advance Manufacturing Technology manuscript No.
(will be inserted by the editor)

In-situ Quality Control of the Selective Laser Melting Process using a High Speed, Real-Time Melt Pool Monitoring System

S.Clijsters · T. Craeghs · S. Buls · K. Kempen · J.-P. Kruth

Received: date / Accepted: date

Abstract This paper discusses the principle and the relevance of an in-situ monitoring system for Selective Laser Melting (SLM). This system enables the operator to monitor the quality of the SLM job on-line and estimate the quality of the part accordingly. The monitoring system consists of two major developments in hardware and software. The first development, essential for a suitable monitoring system, is the design of a complete optical sensor set-up. This set-up is equipped with two commercially available optical sensors connected to a FPGA which communicates directly with the machine control unit. While the sensors ensure a high quality measurement of the melt pool, the FPGA's main task is

S.Clijsters · S. Buls · K. Kempen · J.-P. Kruth

Division PMA, Department of Mechanical Engineering, Celestijnenlaan 300B, 3001 Heverlee, Belgium

E-mail: Stijn.Clijsters@kuleuven.be

T. Craeghs

Materialise, Technologielaan 15, 3001 Leuven, Belgium

to transfer the images from the sensors into relevant values at high sample rates (above 10kHz). The second development is the data analysis system to translate and visualize measured sensor values in the format of interpretable process quality images. The visualization is mainly done by a 'Mapping algorithm', which transfers the measurements from a time-domain into a position-domain representation. Further off-line experiments illustrate an excellent compatibility between the in-situ monitoring and the actual quality of the products. The resulting images coming out of this model, illustrate melt pool variations which can be linked to pores that are present in the parts.

Keywords Process monitoring · Selective Laser Melting · FPGA · High Speed · Real-Time

1 Introduction

Selective Laser Melting (SLM) is an Additive Manufacturing technique which is able to produce complex metallic parts from powder materials. The translation of a complex three-dimensional part into layers of two-dimensions stacked on each other simplifies the job drastically and eliminates the need for die design and tooling. Since material properties of SLM parts are nowadays comparable and even better than the properties of the corresponding bulk material, applications of the process can be found in diverse domains, such as the medical sector [**?**], tool making, automotive, aerospace and general manufacturing industries [**?**,**?**,**?**,**?**,**?**].

The principle of the process is a relatively simple cycle of two actions. In a first step a thin layer of metal powder (20-150 μm) is deposited by means of a powder deposition system. In the second step a laser melts the powder according

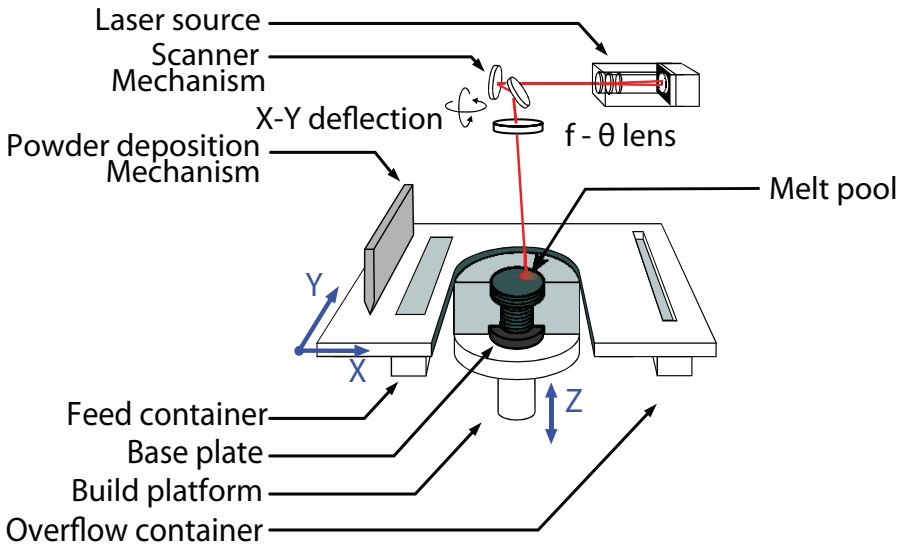

Fig. 1 Schematic overview of the SLM Process

to a predefined scanning path [**?**]. This scanning path is a line pattern generated to fill the two-dimensional layer contours extracted from the three-dimensional CAD model. Once the layer is scanned by the laser, the part is lowered one layer-thickness and the cycle can repeat itself. A schematic overview of the process is illustrated in figure 1.

Due to the very local laser heat input, the material will be different in comparison to conventional production techniques for bulk materials, such as casting or extrusion. The localized heat input, induced by the laser, results in a high thermal gradient in space and time, creating thermal stresses. Thermal stresses can induce deformations which can even cause a job to fail [**?**,**?**]. The high cooling rates result in a very fine microstructure, influencing the mechanical performances of the product [**?**].

In recent years the SLM process technology evolved drastically in machine construction, production speed, expansion of the material palette and part quality, due to the increasing interest of the market. However, for a large breakthrough of SLM in industries with high quality demands, an important issue to be addressed is quality control [**?**]. Problems occurring during the process can result in job failure, create porosities or other defects. Due to the layer-wise nature of the process these defects will not always be visible once the part production is completed. To ensure the internal quality, some components are tested with X-ray Computed Tomography (CT). However since CT is still not widely used due to the limited accuracy, the limitation in part size and the high cost, this is not a standard applied quality assurance method.

By introducing an on-line process monitoring system the part quality can be monitored during the build. This allows the operator to assure the quality of the part without the use of expensive CT measurements. At a later stage it may even enable the implementation of automatic in-process corrective actions to increase the robustness of the process. These on-line parameter adaptations can enhance the likeliness of successful production. This is obviously advantageous to off-line and a posteriori quality control which does not allow immediate in-process corrective measures if the quality of the part does not reach the standard.

In this paper the in-situ monitoring system of KU Leuven installed on its in-house built SLM machine is explained into detail. The principle and the output of this system with examples provided of detectable features/failures are discussed. This covers the full chain from sensing to interpretation of the sensor values. The monitoring delivers crucial information to better understand the process and

opens possibilities for automated quality and feedback control to increase process robustness.

Similar optical hardware set-ups have been developed by other research institutes based on their needs and interest, for example the monitoring set-up of Lott et al. [**?**]. This coaxial set-up, is similar to the optical set-up discussed in detail below. However the set-up of Lott is expanded with an illumination laser beam (laser beam with a different wavelength than the powerful laser used for melting) in order to visualize the melt pool dynamics. By adding this laser the intensity of the reflected light beam is higher. This enables the camera to capture images at high sample rates. This is necessary for visualizing the melt pool dynamics.

Another interesting set-up is the one developed by Doubenskaia et al. [**?**,**?**]. They use a home developed pyrometer consisting of two photodiodes in the range of 900-1700nm. This sensor is not only able to give a relative indication of the melt pool temperature but is also able to measure the absolute temperature. To do this the sensors were calibrated with a W-lamp. Besides the development of the set-up a lot of research on the influence of different process parameters is conducted by them, showing very interesting results on the melt pool behavior due to heat conductivity.

All these systems show a lot of similarities, for instance the coaxial set-up, however most systems do not sample signals at high rates and/or interpret them immediately (in Real-Time). These things are necessary to implement Real-Time feedback control. Besides the Real-Time, the measured signals in all the systems found in literature are measured and visualized in time. This makes the interpretation of these sensor values difficult. Therefore in current developed system the position is sampled together with the melt pool sensor values, to open up new

possibilities of data visualization and interpretation. These new interpretation and visualization enables to detect pores bigger than $100\mu m$.

2 Experimental set-up

The implementation of a monitoring system demands full access to the machine's hardware and software. The in-house developed SLM machine of KU Leuven was therefore equipped with this set-up. This machine distinguishes itself from commercial machines, by besides the full access to the hardware, its in-house developed machine control system. This system is implemented on a National Instruments PXI system (real-time PC system extended for instrumentation) equipped with a dedicated FPGA[1] for the image processing of camera frames. Processing data on a FPGA, opens possibilities for high sample rates ($\geq$ 10kHz) and real-time interaction. The SLM machine is equipped with an Ytterbium (Yb) fiber laser with a wavelength of 1064nm and maximum output power of 300W. The focused laser beam has a spot diameter of 80 μm (ϕ_{1/e^2}) on the building plane.

The monitoring set-up is constructed out of four elements. The optical set-up is the first one, consisting of all optical components and sensors. This set-up sends its sensor data towards the second component, which is the data processing unit (implemented on FPGA). This second unit will calculate melt pool area or other parameters from the image frames and is part of the hardware set-up together with the optical set-up. The processed data will be evaluated and compared to reference data generated by the third module. Such reference data is the expected sensor value of the melt pool. This comparison to the reference data and interpretation of

[1] Field Programmable Gate Array

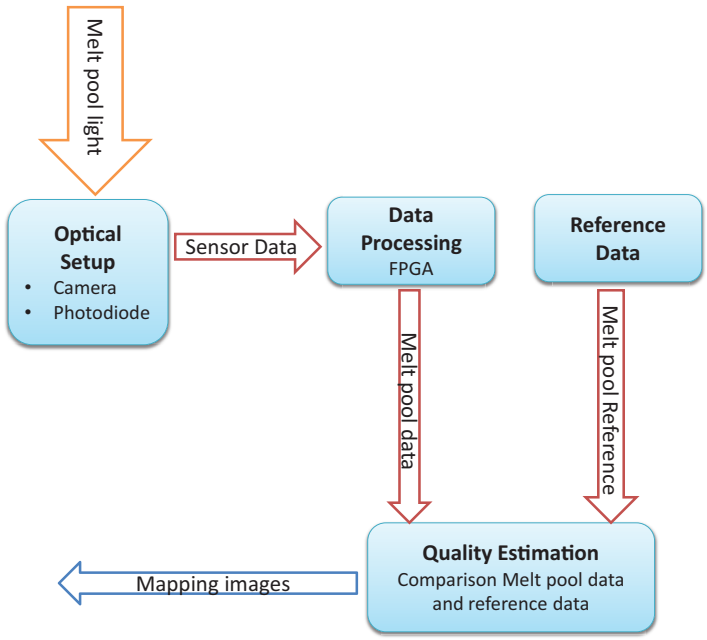

Fig. 2 A schematic overview of the complete experimental set-up of the monitoring system

the signals is done in the fourth and last component (which is the most important software component). This unit estimates the quality and presents it in a map for each layer (explained in section 2.4 Estimating the quality). This set-up is shown in figure 2. In the following paragraphs each of these components are explained in detail.

2.1 Optical set-up

The developed optical set-up, described in this section, is characterized by a high speed near-infrared (NIR) thermal CMOS camera and a photodiode coaxial with the laser beam [**?**]. A semipermeable mirror is used to reflect the laser beam towards the scanning mechanism and to enable the sensors to measure coaxial

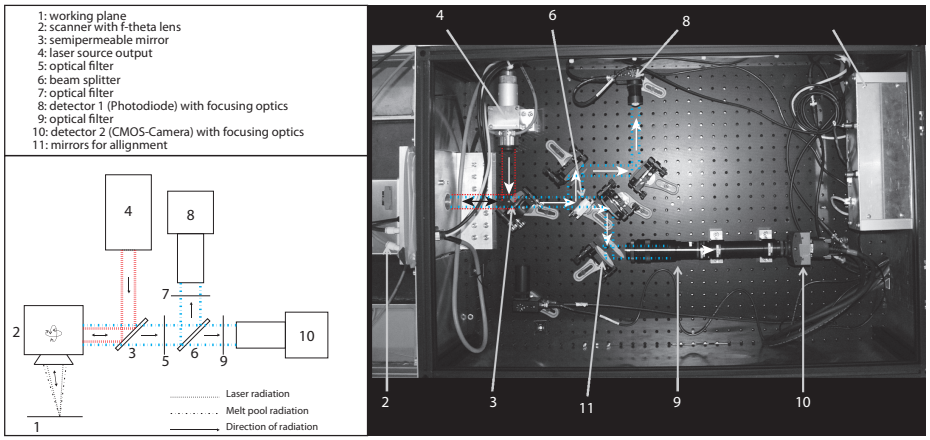

Fig. 3 Optical set-up of the monitoring system

with the laser beam. The full set-up is illustrated in figure 3. The aim of this system is to sample the melt pool at a sample rate of at least 10kHz. This means that for scanning at a speed of 1000mm/s and sampling at 10kHz, every 100μm a sample/picture is taken. This is sufficient since the melt pool diameter is estimated to be around 120μm.

In the optical set-up two different light streams can be distinguished. The first light stream is the high power laserbeam (1064nm), which has to be reflected from the laser source onto the building plate. The second light stream (780-900nm) is the emitted light from the melt pool. This light has to be captured by the sensors. Both light streams are visualized in figure 3.

The first light stream (dotted lines in figure 3) indicates the laser beam. This beam enters the monitoring system through the collimator (4) and is then reflected to the scanning mechanism (2) by a semipermeable mirror (3). The scanning mechanism reflects the beam under a specific angle, which is translated by the f-θ lens into a movement of the laser's focus on the building plane. Powder will selectively be melted on the building plane by controlling the reflection angles.

The second light stream (dot-dash lines in figure 3)is the emitted radiation of the melt pool. This light will track back the laser beam path, through the f-θ lens and the scanning mechanism, (in the opposite direction), until it reaches the semipermeable mirror (3). This mirror reflects the light at the wavelengths around the 1064nm towards the laser source. Light at other wavelengths will pass through the mirror towards a beam splitter (6). After splitting the beam, the radiation beam is sent to each sensor. Both photodiode (8) and camera (9) are sensitive to wavelengths in the range of 400-1000nm.

The selection of optics and filters is extremely important to avoid aberrations in the image and to ensure a high intensity of melt pool radiation. Planck's law states indicates that the radiation energy at the melting point of metals (roughly between 1000 and 2000 degree celsius) contains its peak within the near infrared region (figure 4), between 0.8 and 3μm. However capturing light at these peak wavelengths for monitoring is impossible due to the reflectivity of the semipermeable mirror coated for 1000 nm which reflects almost 100 percent of these wavelengths. Therefore the melt pool radiation can only be captured in a range of wavelengths at a certain spectral distance from the laser beam (which is 1064 nm for the Yb fiber laser used in the current set-up).

The captured region of wavelength is selected below 1000nm to increase the dynamical range. Within this range the change of temperature has a stronger impact on the measured signal (as shown in figure 4). The disadvantage of this region is that the emitted light intensity is rather low in comparison to the region above 1000nm. To avoid reflections of these interesting wavelengths by the semipermeable mirror towards the laser, the mirror is coated to pass wavelengths below 950nm which can easily be captured by the sensors. The lower bound of wavelengths that

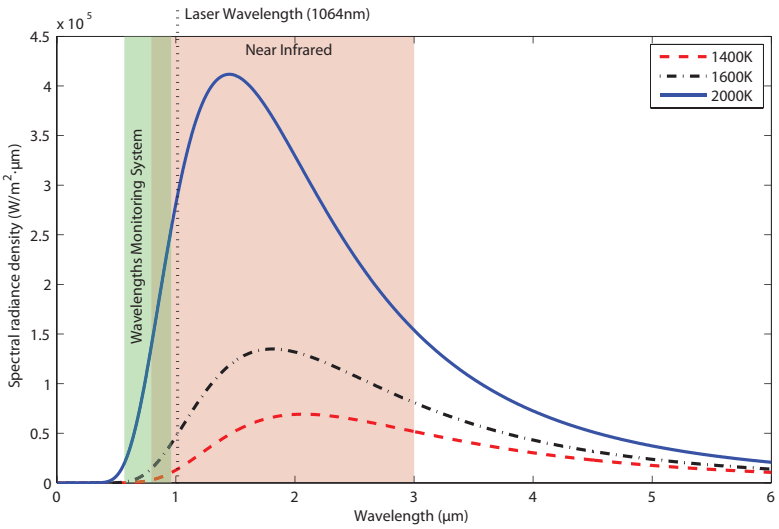

Fig. 4 The different intensity of the emission with different temperatures from a black body (Planck's law)

may pass should be at least 700 nm to eliminate irrelevant visible light (from e.g. illumination in the process chamber) which causes measurements deviations. Nevertheless, the lower bound was selected as 780 nm by using optical filters (5). This limits the aberrations induced by the f-θ lens designed for a wavelength of 1064 nm. Accordingly, a bandwidth of 780 nm to 950 nm is selected as a good trade-off between the different demands (figure 4) which is still large enough to allow the sensors to capture adequate light. The adequate light is necessary to reach the sample rate of 10 kHz. When high scanning speed is used in the SLM process, the sample rate should be higher than 10kHz. In such cases, due to the high intensity of the emitted light, the shutter time of the camera is reduced and the logging speed is increased up to 20 kHz. As shown in figure 4 the intensity of the emitted light also depends on the temperature of the melt pool. This phenomenon has a positive effect on the logging process.

The optical monitoring set-up is equipped with two commercially available sensors. The first one is a planar photodiode sensor including an amplifier. This sensor has a sensing area of $13mm^2$ and a responsivity of $0.45A/W$ in the used wavelength spectrum (780nm-950nm). This sensor can reach a bandwidth up to 10MHz for the lowest amplification level. The main advantage of this sensor is the fact that it absorbs the radiation coming from all points of the melt pool and integrates it into one sensor value representing the melt pool size (area). This benefit is also the limitation of this sensor, which allows only one sensor value to characterize the melt pool. Therefore the monitoring system is equipped with another sensor.

This second sensor is a commercially available CMOS camera and has the possibility to capture the geometry of the melt pool. This camera is equipped with a 1280x1024 pixel CMOS sensor and has a full CameraLink Interface. The sensor can sample at a maximum framerate of 500fps for 1280x1024 pixels and above 10,000fps working with a reduced region of interest. A custom designed lens is placed in front of the camera which consists of several different optical components to provide a zooming function and eliminate the aberrations of the f-θ lens. These functions are necessary to ensure high quality images of the melt pool. The sensitivity of the camera is approximately $4000(V/s)/(W/m^2)$ in the wavelength region of 780nm to 950nm. Monitoring the geometry of the melt pool with a camera creates perspectives to calculate the length, width, area, etc. of the melt pool. Provision of geometrical info on the melt pool is the main benefit of this sensor compared to the photodiode. However due to image processing calculations and mainly the low sensitivity of the camera, this sensor is slower than the photodiode. The camera is connected to the FPGA by a full CameraLink connection, used for

the image processing. This will be explained more into detail in subsection 2.2 Data Processing.

2.2 Data Processing

This section discusses data processing according to the sensor values of the optical set-up. Logging data of a photodiode and a CMOS-camera at high speed demands a dedicated implementation, especially with the aim to implement feedback control in the near future.

To enable feedback control, analyzed sensor data should be available at high sample rates. Those high sample rates can only be reached by having fast sensors and a fast data processing tool. In practice, most image analysis systems store the captured images in memory. Afterwards, a dedicated image processing software should analyze the stored images. This is a rather slow process. For example, if the camera samples images of 60 $\times$ 60 pixels at 10kHz, it results in a continuous data transfer stream of 36 Megabytes/second (1 byte/pixel $\times$ 3600 pixels/image $\times$ 10000 images/second) (excluding the overhead). Then, the software starts loading the image and executes the calculations. These two actions take more than 0.1μs (10kHz).

The relatively slow speed of such a system indicates that a different data processing implementation must be selected. For this purpose, a FPGA chip is chosen to reach the maximum data analysis speed with state-of-the-art technology in image processing. Such a FPGA chip provides fast and robsut calculations in hardware. By this implementing method the lead time from image capture till 'sensor' value is gone. When the last data bit of the image enters the FPGA,

one clock cycle later (40MHz) the processed sensor signal leaves towards the controller. However, the main difficulty in using FPGA's is the programming of such a chip. Conventional FPGA programmers commonly use a programming language called VHDL, which is hard to master and debug. Alternatively, labVIEW can be used instead (which is applied in this work) as a user-friendly and sustainable programming language.

By using this FPGA chip, following melt pool 'sensor' values can be read (from the photodiode) or calculated (on the camera image):

1. **Melt pool intensity (photodiode signal (V)):** amount of light emitted by the laser heated zone and captured by the photodiode
2. **Melt pool area (camera signal (pixels)):** amount of pixels above a certain brightness level[2]
3. **Melt pool length (camera signal (pixels)):** maximum pixel count in a thresholded heated zone parallel to the scan direction
4. **Melt pool width (camera signal (pixels)):** maximum pixel count in a thresholded heated zone perpendicular to the scan direction

These sensor values can be logged for quality control or for feedback control in future research. It should be noted that these values are not absolute values and are only an indication of the melt pool size. However, they can still be used as a good indication for the melt pool stability and quality.

The following sections on Reference Data and Estimating the quality are all implemented in software components. This implementation of the method for analyzing and visualizing the data is necessary to predict the quality of parts.

[2] The level of brightness is determined by the amount of energy absorbed by a pixel. This energy intensity is function of the temperature, material, phase, ...

2.3 Reference Data

The technical details of the optical set-up and data processing has been explained in previous sections. In this section the focus is on the data interpretation. Monitoring the melt pool during the process allows the machine to detect variations in melt pool dimensions. These variations are a result of the melt pool dynamics or can be assigned to disturbances of external factors; such as bad powder layer deposition, dirt on the laser optics, to much oxygen in the inert chamber, irregular heat transfer due to the geometry of the part, etc.

All these external disturbances are difficult to measure or to predict. Only the influence of the geometry of the produced part can be taken into account by proper job preparation and interpretation. To create an accurate quality control, it is therefore important to take the geometry into account to properly predict these variations. This can be done by creating position dependent reference data. This reference data is the sensor values that are expected during the process on a specified location for the creation of a high quality and dense part.

This reference data is determined by the geometrical location in the part and can be generated by two empirical methods. The first method is only applicable for series production, which makes the method very suitable for aerospace applications. To generate the reference data, the parts of small series production are built 5 times. These parts will then be checked and validated on their quality by traditional validation techniques (CMM, CT, archimedes, microscope, etc.). If these parts fulfill the quality requirements, the logged data can be used as a reference.

Since this previous method is only applicable for series, another method was designed based on the local geometrical properties being scanned by the laser.

This method classifies all scanning vectors depending on their heat flow situation and/or properties such as accuracy and roughness and defines reference data based on these properties. Comparing the measurements of the vectors to the reference data of the same class build up in a database, gives . Since this method is applicable to every part, it is more suitable for unique parts. Since this method is of bigger scientific interest, this paper focuses on this method.

To generate reference data dependent on the geometrical location, it is critical to log the vector location and its sensor value. Besides the location it is also crucial to store the parameter settings used for the vector. The parameters for scanning a contour are different than filling the center of a part and can therefore be defined in different vector types. These vector types can be classified according to different heat transfer situations (like small features such as thin walls) and/or different product properties (e.g. roughness, accuracy, etc.). For different vector types different parameter sets are used to optimize the melt process (e.g. contour scan parameters are developed for high accuracy while fill parameter sets are designed for high productivity). Some specific examples of research on distinguishing vector types and determining optimal parameters can be found in [**?**,**?**,**?**]).

Figure 5 shows two different heat flow situations / vector classes, i.e. the heat flow of scan tracks on solid substrate for both contour and fill scans. The classification is determined by the amount of solid material around the melt pool (influencing the heat flow) as well as the required physical and dimensional properties of the part in this scan zone. The contour is scanned with low power and low scanning speed to improve the accuracy, while the fill scans are adjusted to high power and high scanning speed to increase the productivity. In this example the contour is scanned before filling the part.

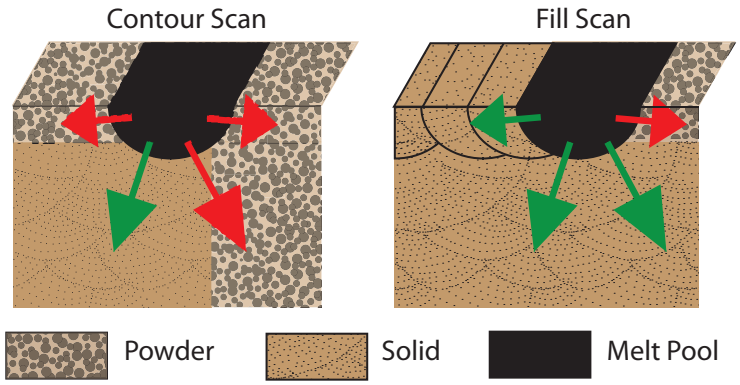

Fig. 5 The different scan vector classes. (Green = high heat flux due to solid material, Red = low heat flux resulting from the isolating properties of powder)

Figure 6 shows the relative histogram distribution of the melt pool size for two different heat flow situations 5 measured by the camera. It can be seen that the optimal melt pool area is different for the demonstrated situations. The pixel value (in figure 6) is a characterization parameter of the melt pool. The interpretation and explanation of the data and units will be explained and linked to the quality of the part in the following sections.

2.4 Estimating the quality

Once sensor values have been collected during a new build job (i.e. after reference data has been collected during reference build jobs), a good visualization is necessary to simplify the interpretation of these sensor values. To do so, the sensor values are not visualized in time, but according to their logged positions. This enables failure detection at certain locations of a part. To visualize in space an algorithm called “mapping” is developed and implemented.

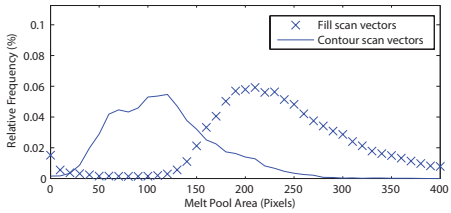

Fig. 6 Relative histogram of melt pool area signal for different scan vector classes

The mapping algorithm transfers a set of x-, y-positions and one of the sensor values into a 2D map (this algorithm is illustrated for one scan vector in figure 7). The measured melt pool data are mapped on a regular grid. Thus, all melt pool data are assigned to the pixel which is closest to the corresponding measured position. When more than one data point is assigned to a pixel, the average of all data inside the pixel is taken. So for every layer a two dimensional picture

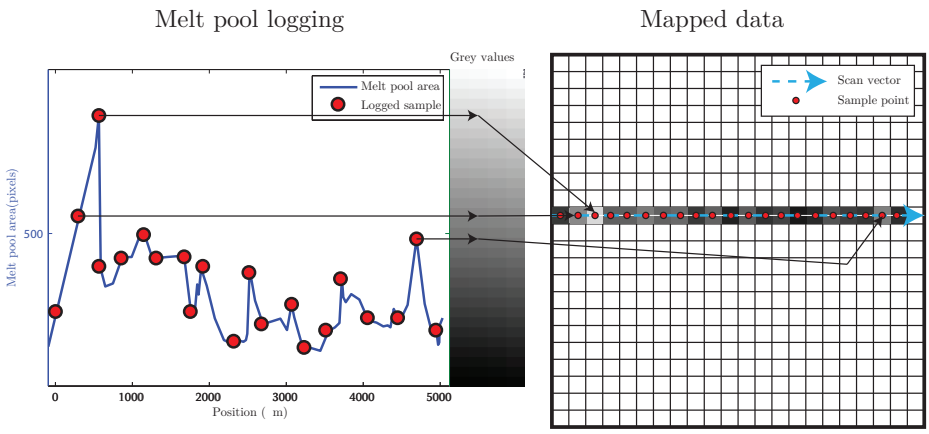

Fig. 7 Illustration and schematic interpretation of the mapping algorithm for one scan vector. At the left side the measured melt pool values are visible. These sensor values can be correlated to a grey value. These grey values can then be plotted on a regular grid. If this is done for each vector of a layer on one grid a mapping of a complete layer will be generated.

is constructed, consisting of 'pixels'. Assembling all mapped layers results in a three-dimensional 'voxel' model.

3 Experimental Results and Discussion

In this section data captured by the monitoring system will be used to detect errors and estimate the part quality. The data of the melt pool intensity (photodiode signal) and the melt pool area (CMOS camera) are visualized with the mapping algorithm, which is a position based visualization method.

In the first part of the results and discussion, the selection of correct reference values by steady-state melt pool measurements is explained. After this section the detection of errors is discussed.

3.1 Steady State Melt Pool Measurements

This section focuses on quality assessment of the measured melt pool. To validate the quality it is essential to have expected sensor values of the melt pool predefined. Such a reference value is predicted from empirical results.

Figure 6 displays relative frequency histograms of the melt pool area for fill and contour scan vectors. Accordingly, the population of the sensor values of these vectors can be used to calculate statistical parameters such as the mean value and standard deviation of the population distribution for a certain vector class. In addition to these standard statistical parameters, a confidence interval can be calculated on this reference data, which can simplify the interpretation process. In figure 8 the cumulative relative frequency distribution of fill scan vectors are illustrated together with the empirically defined 95% confidence interval. This confidence interval is the basis for quality estimation.

The determination of the confidence interval is a simple procedure. By plotting a relative cumulative frequency distribution of a vector type, the boundaries for, for example 95% confidence interval can be defined as a range that includes 95% of the data population. It is worth mentioning that the distribution of the melt pool sensor values are not Gaussian due to the transient behavior at the start and end of a vector and therefore it is preferable to define a confidence interval with experimental data of which the density is validated (as suggested in 2.3 Reference Data). This can be repeated for all different vector types and each sensor value to achieve a complete and reliable quality control system.

The statistical analysis above were performed only on the melt pool intensity (photodiode) and on the melt pool area (CMOS camera) (figure 6), for two vector

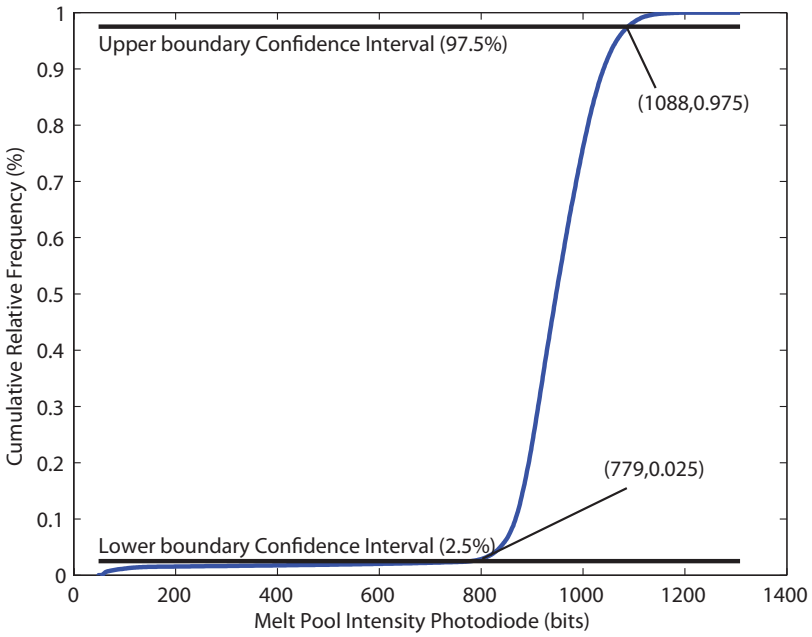

Fig. 8 Cumulative relative frequency distribution of fill scan vectors TiAl6V4

Table 1 Reference values of fill and contour scan vectors achieved for SLM of Ti6Al4V

Sensor	Vector	Mean Value	Conf. Interval
Area	Fill	261 pixels	[135;488] pixels
Area	Contour	118 pixels	[43; 214] pixels
Intensity	Fill	938 bits	[779; 1088] bits
Intensity	Contour	209 bits	[178; 250] bits

types: contour and fill vectors. For each material empirical values have to be tested and validated. The example material in this paper is Ti6Al4V. The mean values and confidence intervals of these analyszes can be found in table 1.

As can be seen in table 1, the values for contour scans are smaller than these for the fill scans despite the fact that contour scans have less heat flow than fill scans. This is due to the fact that for contour scans a lower scan speed en laser power is

used to have a better accuracy. It can be seen that the melt pool for contours has a much smaller confidence interval then for the fill vectors. This smaller confidence interval due to the fact that for contour scans more measurements are made during the steady state scanning of the melt pool. In case of high speed fill scans the ratio of melt pool in transient state to melt pool in steady state is much higher in comparison with contour scans. This results in more loggings in transient state which increases the standard deviation.

It would be possible by future research to filter out these measurements in transient states (e.g. forming of melt pool, small overheating, ...) to have more accurate reference values and a smaller confidence interval for steady state. However this means that new vector classes for each transient state, during the formation of a melt pool, should be defined. This necessitates new reference values and confidence interval (which should be empirically tested and calculated) for each new vector class.

3.2 Overheating of the Melt Pool

Melt pool overheating is one of the most common problems in SLM. This problem occurs due to an increase in heat input at a certain location. This can be due to scanner dynamics, laser instability or other phenomena. The overheating results in an increase in melt pool size and intensity and raises the melt pool turbulence and material evaporation. The excessive turbulence/evaporation could result in the formation of spherical pores and should therefore be kept to a minimal level. In the following paragraph an example of overheating is explained.

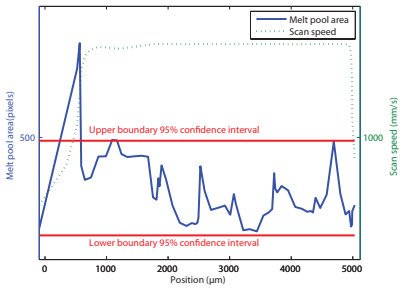

(a) Melt pool area (CMOS) of fill laser scan of a Ti6Al4V cube with high power

(b) Result of overheating in the beginning of the fill vector

Fig. 9 Example of overheating during SLM of Ti6Al4V

In this work, the melt pool behavior is monitored to detect unwanted phenomena. Since the expected variations are defined (based on their vector type as mentioned in 2.3 Reference Data), it is feasible to detect a defect when the melt pool sensors measure a value outside the confidence intervals due to any unwanted phenomenon. Figure 9(a) shows a typical graph of the melt pool for fill scan vector during the scanning of a cube. The used parameters were a laser power of 250W and a scanning speed of 1600mm/s. The dynamic response of the optical scan system, however, is not infinitely fast and undergoes a time interval before it reaches the full operational condition. In other words, scanning requires a certain amount of acceleration time to reach the required scanning speed. This results in low part quality in locations where non-optimal conditions were applied. The acceleration time affects the beginning of a vector and reduces the quality of the

part at the edges (e.g. by formation of porosity). This can deteriorate the fatigue properties of the part (which are very sensitive to surface conditions). Scanning at lower speed than expected, in conjunction with the high laser power (optimised for a high scanning speed), results in excessive heat input around the beginning of the vector. This surplus of heat enlarges the melt pool at the edges which may consequently lead to excessive flow turbulence and evaporation. For instance figure 9(a) illustrates the confidence interval of 95%, determined on the steady state melt pool properties (see section 3.1 Steady State Melt Pool Measurements). The melt pool area captured by the camera clearly steps outside the confidence interval in the beginning of the vector. This indicates that the process is not acting as expected.

Resulting from this irregularity porosity forms at the beginning of the vector. Once the scanning reaches the optimum defined scanning speed, the melt pool size becomes stable (figure 9(a)). This drawback can be eliminated by adapting the scan strategy, as done in commercially available "skywriting": i.e. adding an acceleration vector in front of the scan vector to be at nominal speed by the start of the vector, the laser being only switched on at the start of the scan vector.

3.3 Detection of Pore Positions in X,Y-plane

As discussed in the previous section, detecting errors looks rather simple. However, since different scan tracks are overlapping and remelting previous scan tracks, interpreting sensor values only based on time scale can be challenging. Therefore the mapping algorithm is designed and implemented. This algorithm transfers the time based sensor values into interpreted signals on their position in (X,Y)-maps.

Melt pool instability occurring in different scan tracks, on the same location can easily be detected on these mapping figures. As illustrated above, disturbances of the melt pool mostly result in pores. By plotting all the melt pool errors on maps, porosities in a part can be linked to locations where melt pool disturbances commonly occur during the build. An example is illustrated in figure 11.

During the SLM of AlSi10Mg some instabilities were observed due to poorly selected process parameters (laser power and scanning speed). The melt pool became unstable and started to break up. [**?**] The melt pool sensor will measure lower signals. This melt pool variation due to a physical phenomenon indicates that defects are being formed.

To validate this hypothesis, the part was cut parallel with a XY-plane (figure 10(a)), polished and analyzed using an optical microscope. Figure 11 shows the mapping and a polished cross section of the built part. Despite the fact that perfect polishing in one plane is not practically feasible, there is still a clear correlation between the mappings and the microscope images. This indicates the success of the used in-situ quality monitoring.

3.4 Detection of Pores Positions in three dimensions

To ensure the quality of a full part, all data monitored throughout an entire job can be bundled and analyzed together. As shown in previous sections the mappings of a plane can be linked to the porosity in that plane. By stacking the layer mappings on eachother, a 3D voxel model can be generated. This model indicates the quality throughout a full job. This method is very similar to the CT or MRI methods

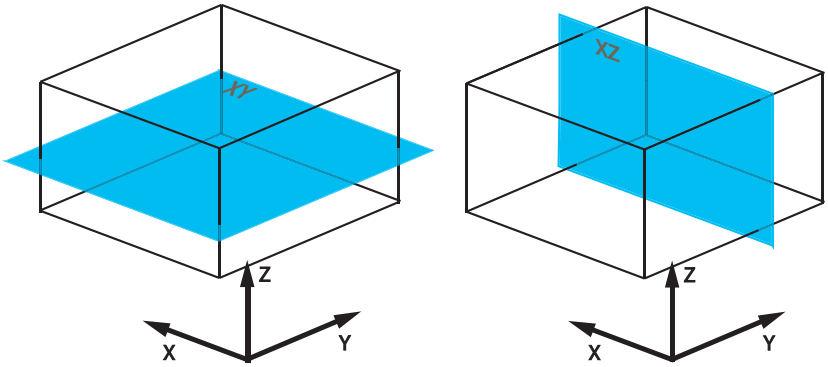

(a) Cutting plane for creating X,Y-plane (b) Cutting plane for creating X,Z-plane

Fig. 10 Cutting planes for creating cross sections of cubic parts (Z-axis is building direction)

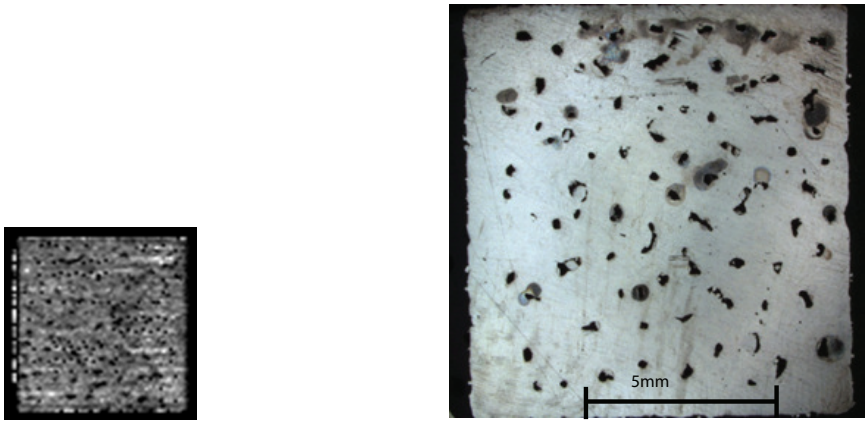

(a) Mapping of the X,Y-plane (b) Microscope image of a X,Y-plane

Fig. 11 Comparison of the mappings and the microscope image of a X,Y-plane

used in medical imaging. By using standard thresholding methods (similar to the confidence intervals) it is possible to detect porosities.

By using medical imaging software such as Mimics, cross sections in any direction can be made. An example of such cross section in the X,Z-plane is illustrated

in figure 12(a). This image is a cross section of all the stacked mappings of the layers. As seen, the porosities in figure 11 are regularly formed. The low sensor values of the melt pool always seems to occur on the same X,Y-position throughout the layers. To validate the in-situ result, the part was cut parallel to the building direction (figure 10(b)) and again the pores were clearly visible (figure 12). These figures show an excellent compatibility between the real microscope images and in-situ mappings. It should be noted that the thresholding algorithm and the confidence intervals of AlSi10Mg still requires further modification by using more empirical data to improve the accuracy. However it is important to notice that pores in the microscopic image are not located on the same locations as on the mappings. The mismatch between the similar X,Z- or X,Y-planes for mapping and microscopic images is due to the polishing of the specimen. Polishing exactly in a known plane is impossible. Both images show similar trends vertical pores in the X,Z-plane and a pore pattern in the X,Y-plane and are expected to match. To validate this some further tests have been conducted to validate the mappings with Computed Tomography.

3.5 Validation

Since it is rather impossible to create microscopic images in a plane that can be reconstructed in the mappings, a different approach to validate the correlation between mappings and pores was tested. This strategy compares the generated mappings with X-ray Computed Tomography. The material used for this validation is NiTinol and AlSi10Mg. By using a reconstructed 3D model from the mappings

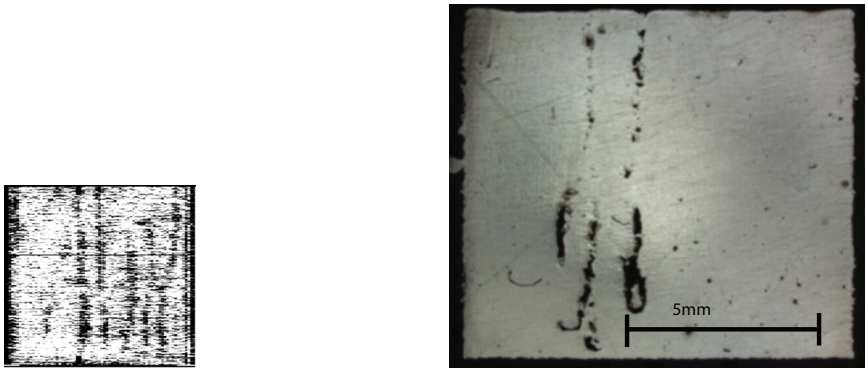

(a) Mapping of the X,Z-plane (b) Microscope image of the X,Z-plane

Fig. 12 Comparison of the mappings and the microscope image of a X,Z-plane

and from the CT measurements, both sample models can be examined on the same location.

Figure 13 shows an example of a cross section in the X,Y-plane of the mappings and the CT model for NiTinol. It is clear that the pore seen in the CT model is induced by the melt pool variation on the mapping image. This indicates that the monitoring system is able to detect defects.

To validate the robustness of the system for different materials, a validation test is also conducted on AlSi10Mg. The correlation between the mappings and pores is visible during the production of a mould with cooling channels (figure 14). Relative big pores marked with a highlighted circle (by a thresholding algorithm) in the CT image can be traced back on the mappings, which show on the same locations a rather dark spot due to melt pool variations. Despite the correlation also other melt pool variations are visible on the mappings which do not induce any

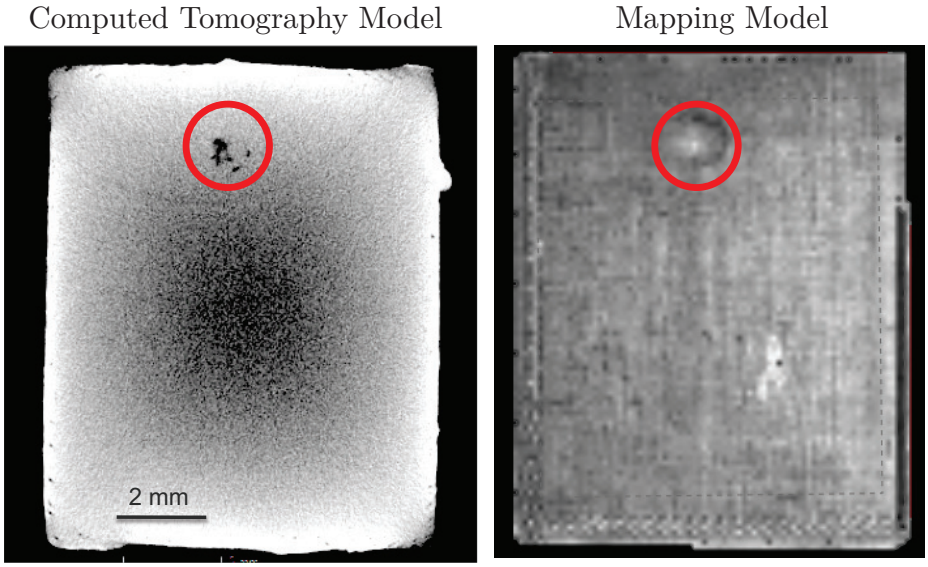

Fig. 13 Comparison of mapping model and X-ray CT model, NiTinol

defects visible on the CT image. Therefore further research needs to be conducted for filtering out irrelevant melt pool variations. By comparing these two models it shows that the monitoring system can be used to detect pores in SLM produced samples. However some more filtering should be developed to enable automatic error detection of a part.

The resolution and accuracy of this quality control system is determined by the mapping algorithm and the sample rate. Currently each pixel of a mapped image is $100\mu m$ by $100\mu m$. The pixel size is selected based on the expected melt pool size (around 120-150μm diameter) and sample rate. Therefore a pixel where the melt pool is mapped will definitely be influenced by the measured melt pool signal. The automatic detection of very small pores (smaller than $100\mu m$) will need, due to the big pixel size, a more complex algorithm than just tresholding.

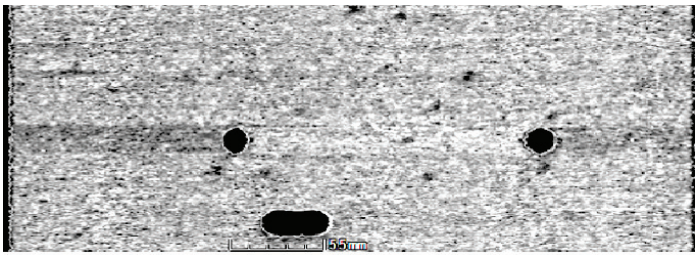

(a) Mapping of the X,Z-plane (AlSi10Mg)

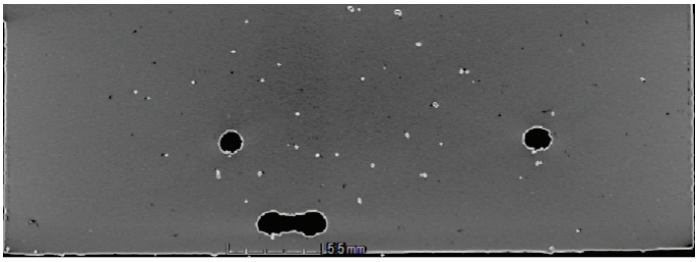

(b) CT crossection image of the X,Z-plane (AlSi10Mg)

Fig. 14 Comparison of the mappings and X-ray CT model (the three big holes are cooling channels) , AlSi10Mg

4 Conclusions

In this work, the in-situ monitoring system on the SLM machine is explained in detail. The set-up consists of a photodiode and a near-infrared thermal CMOS camera together with the data capturing and processing system. This dedicated implementation tool is essential to reach the high requirements for monitoring and logging of melt pool data of the SLM process at high sample rates. This set-up enables the operator of the SLM process to log melt pool intensity, area, length and width, at a sample rate of at least 10kHz and up to 20kHz. These sensor values are even available in real-time to make feedback control possible in the near future.

Afterwards the data processing and interpretation of sensor values are extensively discussed. Vectors are classified into different zones of different heat flow situation and/or different parameter sets. For each of these classes, a confidence interval is defined, which assists the interpretation process of the signals. Once confidence intervals are defined for the different classes, errors can be detected in parts produced by SLM.

The reliability of the in-situ quality control was examined using experimental data after manufacturing parts. The results on Ti6Al4V, AlSi10Mg and NiTinol parts show an excellent compatibility between the actual defects (revealed after cutting the samples or scanning them with X-ray CT) and what is observed from in-situ quality control. Accordingly, the described monitoring system can be successfully employed to reveal the quality of a part during and after manufacturing. It should be noted that the research is still ongoing to enhance the detection resolution of defects such as porosity.

5 Future work

In this work, the principle of the monitoring system is proven to be successful. However, further empirical data (obtained from various materials and manufacturing parameters) is required to extend the confidence intervals for different classes of materials and to improve the robustness of the system. Afterwards, basic algorithms like thresholding together with some filters can be used to automatically detect errors and/or process failures.

Acknowledgements The authors would like to thank Concept Laser GmbH, for the interesting collaboration, discussions and support in this field. Part of the research has received

funding from the European Union's Seventh Framework Program (FP7/2007-2013) under grant agreement number 314055.

International Journal of Advance Manufacturing Technology manuscript No.
(will be inserted by the editor)

In-situ Quality Control of the Selective Laser Melting Process using a High Speed, Real-Time Melt Pool Monitoring System

S.Clijsters · T. Craeghs · S. Buls · K. Kempen · J.-P. Kruth

Received: date / Accepted: date

Abstract This paper discusses the principle and the relevance of an in-situ monitoring system for Selective Laser Melting (SLM). This system enables the operator to monitor the quality of the SLM job on-line and estimate the quality of the part accordingly. The monitoring system consists of two major developments in hardware and software. The first development, essential for a suitable monitoring system, is the design of a complete optical sensor set-up. This set-up is equipped with two commercially available optical sensors connected to a FPGA which communicates directly with the machine control unit. While the sensors ensure a high quality measurement of the melt pool, the FPGA's main task is

S.Clijsters · S. Buls · K. Kempen · J.-P. Kruth

Division PMA, Department of Mechanical Engineering, Celestijnenlaan 300B, 3001 Heverlee, Belgium

E-mail: Stijn.Clijsters@kuleuven.be

T. Craeghs

Materialise, Technologielaan 15, 3001 Leuven, Belgium

to transfer the images from the sensors into relevant values at high sample rates (above 10kHz). The second development is the data analysis system to translate and visualize measured sensor values in the format of interpretable process quality images. The visualization is mainly done by a 'Mapping algorithm', which transfers the measurements from a time-domain into a position-domain representation. Further off-line experiments illustrate an excellent compatibility between the in-situ monitoring and the actual quality of the products. The resulting images coming out of this model, illustrate melt pool variations which can be linked to pores that are present in the parts.

Keywords Process monitoring · Selective Laser Melting · FPGA · High Speed · Real-Time

1 Introduction

Selective Laser Melting (SLM) is an Additive Manufacturing technique which is able to produce complex metallic parts from powder materials. The translation of a complex three-dimensional part into layers of two-dimensions stacked on each other simplifies the job drastically and eliminates the need for die design and tooling. Since material properties of SLM parts are nowadays comparable and even better than the properties of the corresponding bulk material, applications of the process can be found in diverse domains, such as the medical sector [11], tool making, automotive, aerospace and general manufacturing industries [1, 10, 2, 19, 16].

The principle of the process is a relatively simple cycle of two actions. In a first step a thin layer of metal powder (20-150 μm) is deposited by means of a

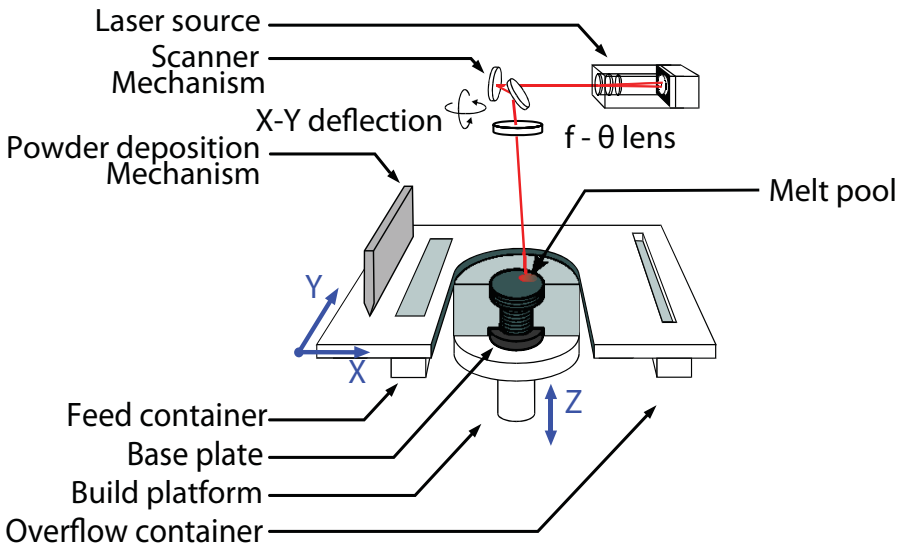

Fig. 1 Schematic overview of the SLM Process

powder deposition system. In the second step a laser melts the powder according to a predefined scanning path [13]. This scanning path is a line pattern generated to fill the two-dimensional layer contours extracted from the three-dimensional CAD model. Once the layer is scanned by the laser, the part is lowered one layer-thickness and the cycle can repeat itself. A schematic overview of the process is illustrated in figure 1.

Due to the very local laser heat input, the material will be different in comparison to conventional production techniques for bulk materials, such as casting or extrusion. The localized heat input, induced by the laser, results in a high thermal gradient in space and time, creating thermal stresses. Thermal stresses can induce deformations which can even cause a job to fail [15,17]. The high cooling rates result in a very fine microstructure, influencing the mechanical performances of the product [18].

In recent years the SLM process technology evolved drastically in machine construction, production speed, expansion of the material palette and part quality, due to the increasing interest of the market. However, for a large breakthrough of SLM in industries with high quality demands, an important issue to be addressed is quality control [3]. Problems occurring during the process can result in job failure, create porosities or other defects. Due to the layer-wise nature of the process these defects will not always be visible once the part production is completed. To ensure the internal quality, some components are tested with X-ray Computed Tomography (CT). However since CT is still not widely used due to the limited accuracy, the limitation in part size and the high cost, this is not a standard applied quality assurance method.

By introducing an on-line process monitoring system the part quality can be monitored during the build. This allows the operator to assure the quality of the part without the use of expensive CT measurements. At a later stage it may even enable the implementation of automatic in-process corrective actions to increase the robustness of the process. These on-line parameter adaptations can enhance the likeliness of successful production. This is obviously advantageous to off-line and a posteriori quality control which does not allow immediate in-process corrective measures if the quality of the part does not reach the standard.

In this paper the in-situ monitoring system of KU Leuven installed on its in-house built SLM machine is explained into detail. The principle and the output of this system with examples provided of detectable features/failures are discussed. This covers the full chain from sensing to interpretation of the sensor values. The monitoring delivers crucial information to better understand the process and

opens possibilities for automated quality and feedback control to increase process robustness.

Similar optical hardware set-ups have been developed by other research institutes based on their needs and interest, for example the monitoring set-up of Lott et al. [14]. This coaxial set-up, is similar to the optical set-up discussed in detail below. However the set-up of Lott is expanded with an illumination laser beam (laser beam with a different wavelength than the powerful laser used for melting) in order to visualize the melt pool dynamics. By adding this laser the intensity of the reflected light beam is higher. This enables the camera to capture images at high sample rates. This is necessary for visualizing the melt pool dynamics.

Another interesting set-up is the one developed by Doubenskaia et al. [4,8]. They use a home developed pyrometer consisting of two photodiodes in the range of 900-1700nm. This sensor is not only able to give a relative indication of the melt pool temperature but is also able to measure the absolute temperature. To do this the sensors were calibrated with a W-lamp. Besides the development of the set-up a lot of research on the influence of different process parameters is conducted by them, showing very interesting results on the melt pool behavior due to heat conductivity.

All these systems show a lot of similarities, for instance the coaxial set-up, however most systems do not sample signals at high rates and/or interpret them immediately (in Real-Time). These things are necessary to implement Real-Time feedback control. Besides the Real-Time, the measured signals in all the systems found in literature are measured and visualized in time. This makes the interpretation of these sensor values difficult. Therefore in current developed system the position is sampled together with the melt pool sensor values, to open up new

possibilities of data visualization and interpretation. These new interpretation and visualization enables to detect pores bigger than $100\mu m$.

2 Experimental set-up

The implementation of a monitoring system demands full access to the machine's hardware and software. The in-house developed SLM machine of KU Leuven was therefore equipped with this set-up. This machine distinguishes itself from commercial machines, by besides the full access to the hardware, its in-house developed machine control system. This system is implemented on a National Instruments PXI system (real-time PC system extended for instrumentation) equipped with a dedicated FPGA[1] for the image processing of camera frames. Processing data on a FPGA, opens possibilities for high sample rates ($\geq$ 10kHz) and real-time interaction. The SLM machine is equipped with an Ytterbium (Yb) fiber laser with a wavelength of 1064nm and maximum output power of 300W. The focused laser beam has a spot diameter of 80 μm (ϕ_{1/e^2}) on the building plane.

The monitoring set-up is constructed out of four elements. The optical set-up is the first one, consisting of all optical components and sensors. This set-up sends its sensor data towards the second component, which is the data processing unit (implemented on FPGA). This second unit will calculate melt pool area or other parameters from the image frames and is part of the hardware set-up together with the optical set-up. The processed data will be evaluated and compared to reference data generated by the third module. Such reference data is the expected sensor value of the melt pool. This comparison to the reference data and interpretation of

[1] Field Programmable Gate Array

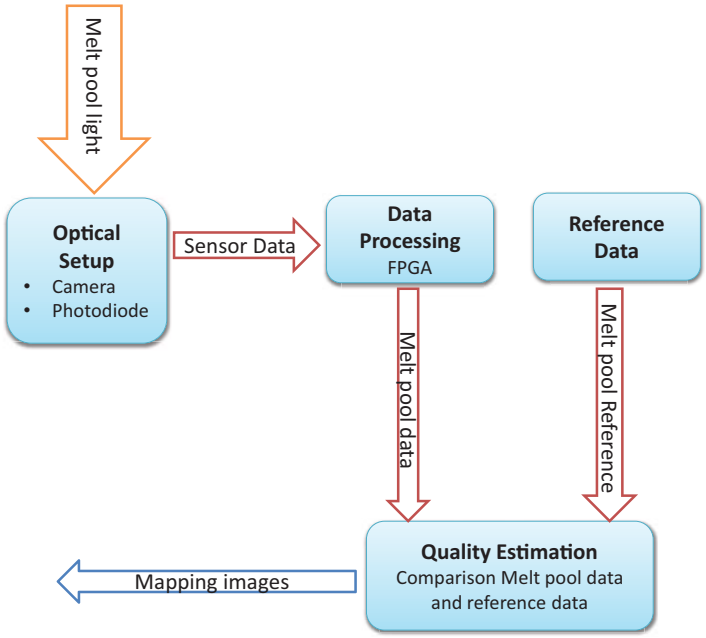

Fig. 2 A schematic overview of the complete experimental set-up of the monitoring system

the signals is done in the fourth and last component (which is the most important software component). This unit estimates the quality and presents it in a map for each layer (explained in section 2.4 Estimating the quality). This set-up is shown in figure 2. In the following paragraphs each of these components are explained in detail.

2.1 Optical set-up

The developed optical set-up, described in this section, is characterized by a high speed near-infrared (NIR) thermal CMOS camera and a photodiode coaxial with the laser beam [7]. A semipermeable mirror is used to reflect the laser beam towards the scanning mechanism and to enable the sensors to measure coaxial with the laser

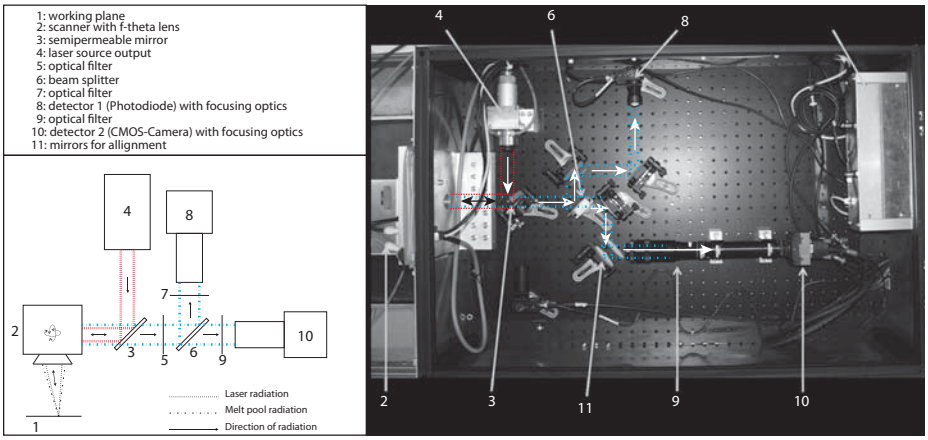

Fig. 3 Optical set-up of the monitoring system

beam. The full set-up is illustrated in figure 3. The aim of this system is to sample the melt pool at a sample rate of at least 10kHz. This means that for scanning at a speed of 1000mm/s and sampling at 10kHz, every 100μm a sample/picture is taken. This is sufficient since the melt pool diameter is estimated to be around 120μm.

In the optical set-up two different light streams can be distinguished. The first light stream is the high power laserbeam (1064nm), which has to be reflected from the laser source onto the building plate. The second light stream (780-900nm) is the emitted light from the melt pool. This light has to be captured by the sensors. Both light streams are visualized in figure 3.

The first light stream (dotted lines in figure 3) indicates the laser beam. This beam enters the monitoring system through the collimator (4) and is then reflected to the scanning mechanism (2) by a semipermeable mirror (3). The scanning mechanism reflects the beam under a specific angle, which is translated by the f-θ lens into a movement of the laser's focus on the building plane. Powder will selectively be melted on the building plane by controlling the reflection angles.

The second light stream (dot-dash lines in figure 3)is the emitted radiation of the melt pool. This light will track back the laser beam path, through the f-θ lens and the scanning mechanism, (in the opposite direction), until it reaches the semipermeable mirror (3). This mirror reflects the light at the wavelengths around the 1064nm towards the laser source. Light at other wavelengths will pass through the mirror towards a beam splitter (6). After splitting the beam, the radiation beam is sent to each sensor. Both photodiode (8) and camera (9) are sensitive to wavelengths in the range of 400-1000nm.

The selection of optics and filters is extremely important to avoid aberrations in the image and to ensure a high intensity of melt pool radiation. Planck's law states indicates that the radiation energy at the melting point of metals (roughly between 1000 and 2000 degree celsius) contains its peak within the near infrared region (figure 4), between 0.8 and 3μm. However capturing light at these peak wavelengths for monitoring is impossible due to the reflectivity of the semipermeable mirror coated for 1000 nm which reflects almost 100 percent of these wavelengths. Therefore the melt pool radiation can only be captured in a range of wavelengths at a certain spectral distance from the laser beam (which is 1064 nm for the Yb fiber laser used in the current set-up).

The captured region of wavelength is selected below 1000nm to increase the dynamical range. Within this range the change of temperature has a stronger impact on the measured signal (as shown in figure 4). The disadvantage of this region is that the emitted light intensity is rather low in comparison to the region above 1000nm. To avoid reflections of these interesting wavelengths by the semipermeable mirror towards the laser, the mirror is coated to pass wavelengths below 950nm which can easily be captured by the sensors. The lower bound of wavelengths that

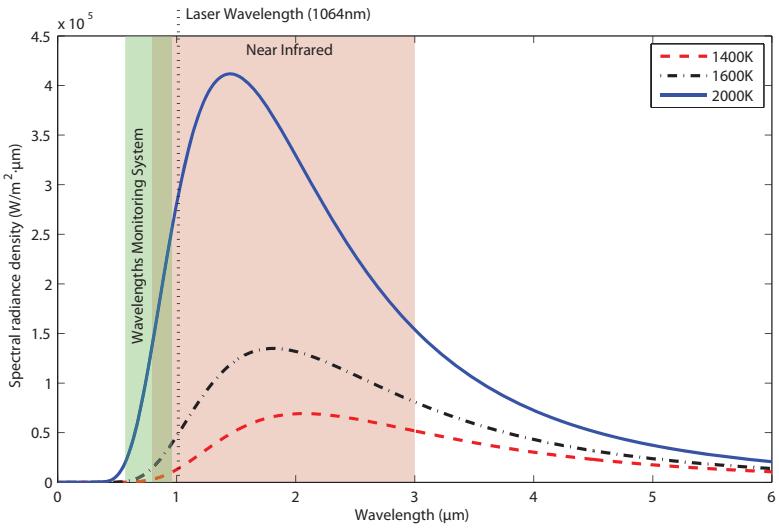

Fig. 4 The different intensity of the emission with different temperatures from a black body (Planck's law)

may pass should be at least 700 nm to eliminate irrelevant visible light (from e.g. illumination in the process chamber) which causes measurements deviations. Nevertheless, the lower bound was selected as 780 nm by using optical filters (5). This limits the aberrations induced by the f-θ lens designed for a wavelength of 1064 nm. Accordingly, a bandwidth of 780 nm to 950 nm is selected as a good trade-off between the different demands (figure 4) which is still large enough to allow the sensors to capture adequate light. The adequate light is necessary to reach the sample rate of 10 kHz. When high scanning speed is used in the SLM process, the sample rate should be higher than 10kHz. In such cases, due to the high intensity of the emitted light, the shutter time of the camera is reduced and the logging speed is increased up to 20 kHz. As shown in figure 4 the intensity of the emitted light also depends on the temperature of the melt pool. This phenomenon has a positive effect on the logging process.

The optical monitoring set-up is equipped with two commercially available sensors. The first one is a planar photodiode sensor including an amplifier. This sensor has a sensing area of $13mm^2$ and a responsivity of $0.45A/W$ in the used wavelength spectrum (780nm-950nm). This sensor can reach a bandwidth up to 10MHz for the lowest amplification level. The main advantage of this sensor is the fact that it absorbs the radiation coming from all points of the melt pool and integrates it into one sensor value representing the melt pool size (area). This benefit is also the limitation of this sensor, which allows only one sensor value to characterize the melt pool. Therefore the monitoring system is equipped with another sensor.

This second sensor is a commercially available CMOS camera and has the possibility to capture the geometry of the melt pool. This camera is equipped with a 1280x1024 pixel CMOS sensor and has a full CameraLink Interface. The sensor can sample at a maximum framerate of 500fps for 1280x1024 pixels and above 10,000fps working with a reduced region of interest. A custom designed lens is placed in front of the camera which consists of several different optical components to provide a zooming function and eliminate the aberrations of the f-θ lens. These functions are necessary to ensure high quality images of the melt pool. The sensitivity of the camera is approximately $4000(V/s)/(W/m^2)$ in the wavelength region of 780nm to 950nm. Monitoring the geometry of the melt pool with a camera creates perspectives to calculate the length, width, area, etc. of the melt pool. Provision of geometrical info on the melt pool is the main benefit of this sensor compared to the photodiode. However due to image processing calculations and mainly the low sensitivity of the camera, this sensor is slower than the photodiode. The camera is connected to the FPGA by a full CameraLink connection, used for

the image processing. This will be explained more into detail in subsection 2.2 Data Processing.

2.2 Data Processing

This section discusses data processing according to the sensor values of the optical set-up. Logging data of a photodiode and a CMOS-camera at high speed demands a dedicated implementation, especially with the aim to implement feedback control in the near future.

To enable feedback control, analyzed sensor data should be available at high sample rates. Those high sample rates can only be reached by having fast sensors and a fast data processing tool. In practice, most image analysis systems store the captured images in memory. Afterwards, a dedicated image processing software should analyze the stored images. This is a rather slow process. For example, if the camera samples images of 60 $\times$ 60 pixels at 10kHz, it results in a continuous data transfer stream of 36 Megabytes/second (1 byte/pixel $\times$ 3600 pixels/image $\times$ 10000 images/second) (excluding the overhead). Then, the software starts loading the image and executes the calculations. These two actions take more than 0.1μs (10kHz).

The relatively slow speed of such a system indicates that a different data processing implementation must be selected. For this purpose, a FPGA chip is chosen to reach the maximum data analysis speed with state-of-the-art technology in image processing. Such a FPGA chip provides fast and robsut calculations in hardware. By this implementing method the lead time from image capture till 'sensor' value is gone. When the last data bit of the image enters the FPGA,

one clock cycle later (40MHz) the processed sensor signal leaves towards the controller. However, the main difficulty in using FPGA's is the programming of such a chip. Conventional FPGA programmers commonly use a programming language called VHDL, which is hard to master and debug. Alternatively, labVIEW can be used instead (which is applied in this work) as a user-friendly and sustainable programming language.

By using this FPGA chip, following melt pool 'sensor' values can be read (from the photodiode) or calculated (on the camera image):

1. **Melt pool intensity (photodiode signal (V)):** amount of light emitted by the laser heated zone and captured by the photodiode
2. **Melt pool area (camera signal (pixels)):** amount of pixels above a certain brightness level[2]
3. **Melt pool length (camera signal (pixels)):** maximum pixel count in a thresholded heated zone parallel to the scan direction
4. **Melt pool width (camera signal (pixels)):** maximum pixel count in a thresholded heated zone perpendicular to the scan direction

These sensor values can be logged for quality control or for feedback control in future research. It should be noted that these values are not absolute values and are only an indication of the melt pool size. However, they can still be used as a good indication for the melt pool stability and quality.

The following sections on Reference Data and Estimating the quality are all implemented in software components. This implementation of the method for analyzing and visualizing the data is necessary to predict the quality of parts.

[2] The level of brightness is determined by the amount of energy absorbed by a pixel. This energy intensity is function of the temperature, material, phase, ...

2.3 Reference Data

The technical details of the optical set-up and data processing has been explained in previous sections. In this section the focus is on the data interpretation. Monitoring the melt pool during the process allows the machine to detect variations in melt pool dimensions. These variations are a result of the melt pool dynamics or can be assigned to disturbances of external factors; such as bad powder layer deposition, dirt on the laser optics, to much oxygen in the inert chamber, irregular heat transfer due to the geometry of the part, etc.

All these external disturbances are difficult to measure or to predict. Only the influence of the geometry of the produced part can be taken into account by proper job preparation and interpretation. To create an accurate quality control, it is therefore important to take the geometry into account to properly predict these variations. This can be done by creating position dependent reference data. This reference data is the sensor values that are expected during the process on a specified location for the creation of a high quality and dense part.

This reference data is determined by the geometrical location in the part and can be generated by two empirical methods. The first method is only applicable for series production, which makes the method very suitable for aerospace applications. To generate the reference data, the parts of small series production are built 5 times. These parts will then be checked and validated on their quality by traditional validation techniques (CMM, CT, archimedes, microscope, etc.). If these parts fulfill the quality requirements, the logged data can be used as a reference.

Since this previous method is only applicable for series, another method was designed based on the local geometrical properties being scanned by the laser.

This method classifies all scanning vectors depending on their heat flow situation and/or properties such as accuracy and roughness and defines reference data based on these properties. Comparing the measurements of the vectors to the reference data of the same class build up in a database, gives . Since this method is applicable to every part, it is more suitable for unique parts. Since this method is of bigger scientific interest, this paper focuses on this method.

To generate reference data dependent on the geometrical location, it is critical to log the vector location and its sensor value. Besides the location it is also crucial to store the parameter settings used for the vector. The parameters for scanning a contour are different than filling the center of a part and can therefore be defined in different vector types. These vector types can be classified according to different heat transfer situations (like small features such as thin walls) and/or different product properties (e.g. roughness, accuracy, etc.). For different vector types different parameter sets are used to optimize the melt process (e.g. contour scan parameters are developed for high accuracy while fill parameter sets are designed for high productivity). Some specific examples of research on distinguishing vector types and determining optimal parameters can be found in [5,6,12]).

Figure 5 shows two different heat flow situations / vector classes, i.e. the heat flow of scan tracks on solid substrate for both contour and fill scans. The classification is determined by the amount of solid material around the melt pool (influencing the heat flow) as well as the required physical and dimensional properties of the part in this scan zone. The contour is scanned with low power and low scanning speed to improve the accuracy, while the fill scans are adjusted to high power and high scanning speed to increase the productivity. In this example the contour is scanned before filling the part.

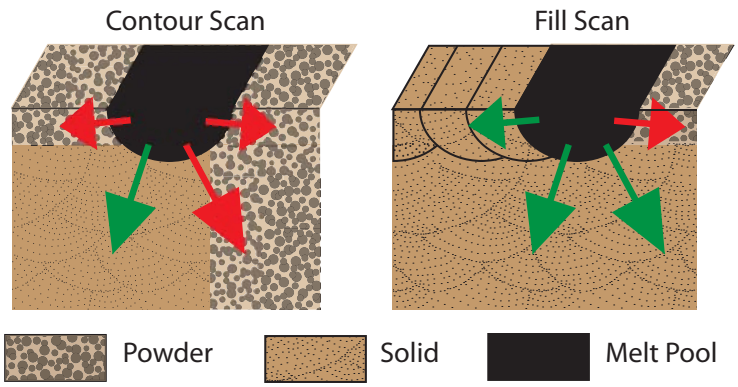

Fig. 5 The different scan vector classes. (Green = high heat flux due to solid material, Red = low heat flux resulting from the isolating properties of powder)

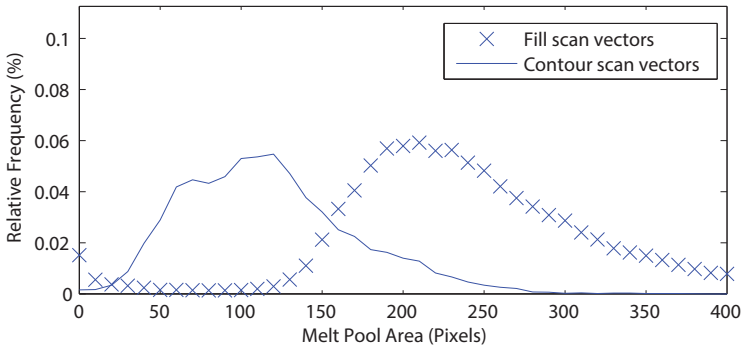

Fig. 6 Relative histogram of melt pool area signal for different scan vector classes

Figure 6 shows the relative histogram distribution of the melt pool size for two different heat flow situations 5 measured by the camera. It can be seen that the optimal melt pool area is different for the demonstrated situations. The pixel value (in figure 6) is a characterization parameter of the melt pool. The interpretation and explanation of the data and units will be explained and linked to the quality of the part in the following sections.

2.4 Estimating the quality

Once sensor values have been collected during a new build job (i.e. after reference data has been collected during reference build jobs), a good visualization is necessary to simplify the interpretation of these sensor values. To do so, the sensor values are not visualized in time, but according to their logged positions. This enables failure detection at certain locations of a part. To visualize in space an algorithm called “mapping” is developed and implemented.

The mapping algorithm transfers a set of x-, y-positions and one of the sensor values into a 2D map (this algorithm is illustrated for one scan vector in figure 7). The measured melt pool data are mapped on a regular grid. Thus, all melt pool data are assigned to the pixel which is closest to the corresponding measured position. When more than one data point is assigned to a pixel, the average of all data inside the pixel is taken. So for every layer a two dimensional picture is constructed, consisting of ’pixels’. Assembling all mapped layers results in a three-dimensional ’voxel’ model.

3 Experimental Results and Discussion

In this section data captured by the monitoring system will be used to detect errors and estimate the part quality. The data of the melt pool intensity (photodiode signal) and the melt pool area (CMOS camera) are visualized with the mapping algorithm, which is a position based visualization method.

In the first part of the results and discussion, the selection of correct reference values by steady-state melt pool measurements is explained. After this section the detection of errors is discussed.

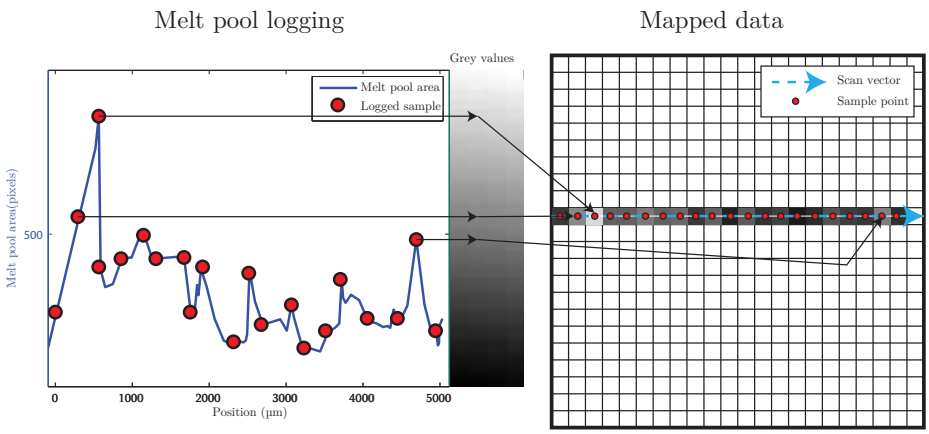

Fig. 7 Illustration and schematic interpretation of the mapping algorithm for one scan vector. At the left side the measured melt pool values are visible. These sensor values can be correlated to a grey value. These grey values can then be plotted on a regular grid. If this is done for each vector of a layer on one grid a mapping of a complete layer will be generated.

3.1 Steady State Melt Pool Measurements

This section focuses on quality assessment of the measured melt pool. To validate the quality it is essential to have expected sensor values of the melt pool predefined. Such a reference value is predicted from empirical results.

Figure 6 displays relative frequency histograms of the melt pool area for fill and contour scan vectors. Accordingly, the population of the sensor values of these vectors can be used to calculate statistical parameters such as the mean value and standard deviation of the population distribution for a certain vector class. In addition to these standard statistical parameters, a confidence interval can be calculated on this reference data, which can simplify the interpretation process. In figure 8 the cumulative relative frequency distribution of fill scan vectors are illustrated together with the empirically defined 95% confidence interval. This confidence interval is the basis for quality estimation.

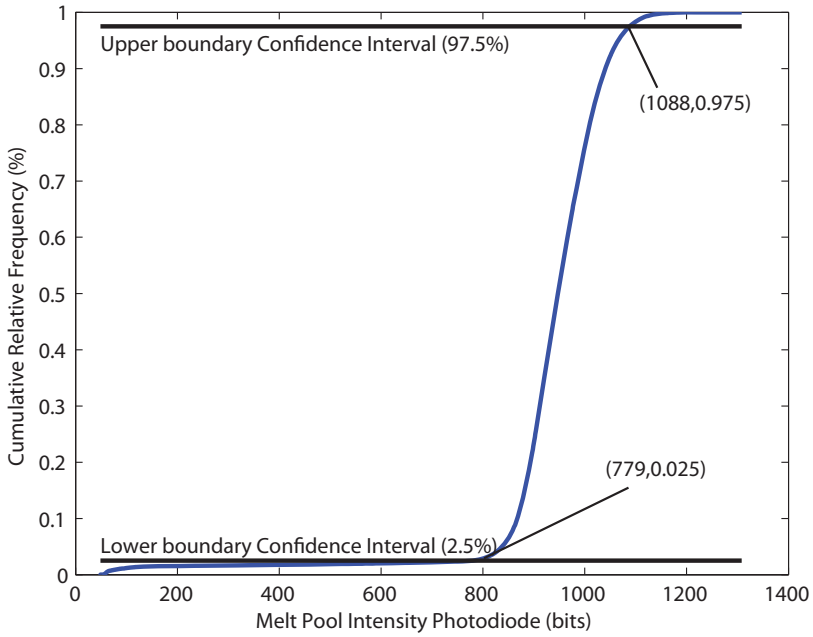

Fig. 8 Cumulative relative frequency distribution of fill scan vectors TiAl6V4

The determination of the confidence interval is a simple procedure. By plotting a relative cumulative frequency distribution of a vector type, the boundaries for, for example 95% confidence interval can be defined as a range that includes 95% of the data population. It is worth mentioning that the distribution of the melt pool sensor values are not Gaussian due to the transient behavior at the start and end of a vector and therefore it is preferable to define a confidence interval with experimental data of which the density is validated (as suggested in 2.3 Reference Data). This can be repeated for all different vector types and each sensor value to achieve a complete and reliable quality control system.

The statistical analysis above were performed only on the melt pool intensity (photodiode) and on the melt pool area (CMOS camera) (figure 6), for two vector

Table 1 Reference values of fill and contour scan vectors achieved for SLM of Ti6Al4V

Sensor	Vector	Mean Value	Conf. Interval
Area	Fill	261 pixels	[135;488] pixels
Area	Contour	118 pixels	[43; 214] pixels
Intensity	Fill	938 bits	[779; 1088] bits
Intensity	Contour	209 bits	[178; 250] bits

types: contour and fill vectors. For each material empirical values have to be tested and validated. The example material in this paper is Ti6Al4V. The mean values and confidence intervals of these analyszes can be found in table 1.

As can be seen in table 1, the values for contour scans are smaller than these for the fill scans despite the fact that contour scans have less heat flow than fill scans. This is due to the fact that for contour scans a lower scan speed en laser power is used to have a better accuracy. It can be seen that the melt pool for contours has a much smaller confidence interval then for the fill vectors. This smaller confidence interval due to the fact that for contour scans more measurements are made during the steady state scanning of the melt pool. In case of high speed fill scans the ratio of melt pool in transient state to melt pool in steady state is much higher in comparison with contour scans. This results in more loggings in transient state which increases the standard deviation.

It would be possible by future research to filter out these measurements in transient states (e.g. forming of melt pool, small overheating, ...) to have more accurate reference values and a smaller confidence interval for steady state. However this means that new vector classes for each transient state, during the formation of a melt pool, should be defined. This necessitates new reference values and con-

fidence interval (which should be empirically tested and calculated) for each new vector class.

3.2 Overheating of the Melt Pool

Melt pool overheating is one of the most common problems in SLM. This problem occurs due to an increase in heat input at a certain location. This can be due to scanner dynamics, laser instability or other phenomena. The overheating results in an increase in melt pool size and intensity and raises the melt pool turbulence and material evaporation. The excessive turbulence/evaporation could result in the formation of spherical pores and should therefore be kept to a minimal level. In the following paragraph an example of overheating is explained.

In this work, the melt pool behavior is monitored to detect unwanted phenomena. Since the expected variations are defined (based on their vector type as mentioned in 2.3 Reference Data), it is feasible to detect a defect when the melt pool sensors measure a value outside the confidence intervals due to any unwanted phenomenon. Figure 9(a) shows a typical graph of the melt pool for fill scan vector during the scanning of a cube. The used parameters were a laser power of 250W and a scanning speed of 1600mm/s. The dynamic response of the optical scan system, however, is not infinitely fast and undergoes a time interval before it reaches the full operational condition. In other words, scanning requires a certain amount of acceleration time to reach the required scanning speed. This results in low part quality in locations where non-optimal conditions were applied. The acceleration time affects the beginning of a vector and reduces the quality of the part at the edges (e.g. by formation of porosity). This can deteriorate the fatigue

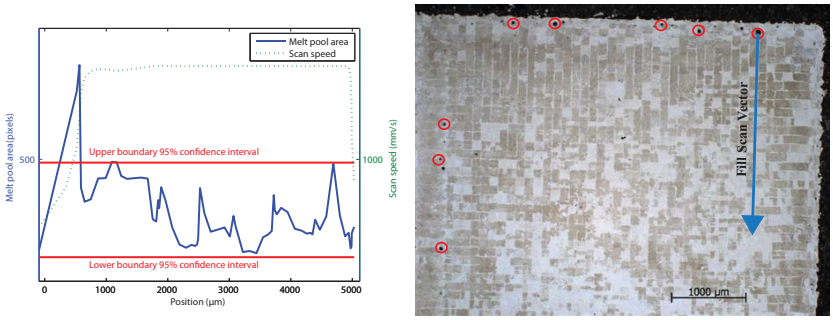

(a) Melt pool area (CMOS) of fill laser scan of a Ti6Al4V cube with high power

(b) Result of overheating in the beginning of the fill vector

Fig. 9 Example of overheating during SLM of Ti6Al4V

properties of the part (which are very sensitive to surface conditions). Scanning at lower speed than expected, in conjunction with the high laser power (optimised for a high scanning speed), results in excessive heat input around the beginning of the vector. This surplus of heat enlarges the melt pool at the edges which may consequently lead to excessive flow turbulence and evaporation. For instance figure 9(a) illustrates the confidence interval of 95%, determined on the steady state melt pool properties (see section 3.1 Steady State Melt Pool Measurements). The melt pool area captured by the camera clearly steps outside the confidence interval in the beginning of the vector. This indicates that the process is not acting as expected.

Resulting from this irregularity porosity forms at the beginning of the vector. Once the scanning reaches the optimum defined scanning speed, the melt pool size becomes stable (figure 9(a)). This drawback can be eliminated by adapting the scan strategy, as done in commercially available “skywriting”: i.e. adding an acceleration vector in front of the scan vector to be at nominal speed by the start of the vector, the laser being only switched on at the start of the scan vector.

3.3 Detection of Pore Positions in X,Y-plane

As discussed in the previous section, detecting errors looks rather simple. However, since different scan tracks are overlapping and remelting previous scan tracks, interpreting sensor values only based on time scale can be challenging. Therefore the mapping algorithm is designed and implemented. This algorithm transfers the time based sensor values into interpreted signals on their position in (X,Y)-maps.

Melt pool instability occurring in different scan tracks, on the same location can easily be detected on these mapping figures. As illustrated above, disturbances of the melt pool mostly result in pores. By plotting all the melt pool errors on maps, porosities in a part can be linked to locations where melt pool disturbances commonly occur during the build. An example is illustrated in figure 11.

During the SLM of AlSi10Mg some instabilities were observed due to poorly selected process parameters (laser power and scanning speed). The melt pool became unstable and started to break up. [9] The melt pool sensor will measure lower signals. This melt pool variation due to a physical phenomenon indicates that defects are being formed.

To validate this hypothesis, the part was cut parallel with a XY-plane (figure 10(a)), polished and analyzed using an optical microscope. Figure 11 shows the mapping and a polished cross section of the built part. Despite the fact that perfect polishing in one plane is not practically feasible, there is still a clear correlation between the mappings and the microscope images. This indicates the success of the used in-situ quality monitoring.

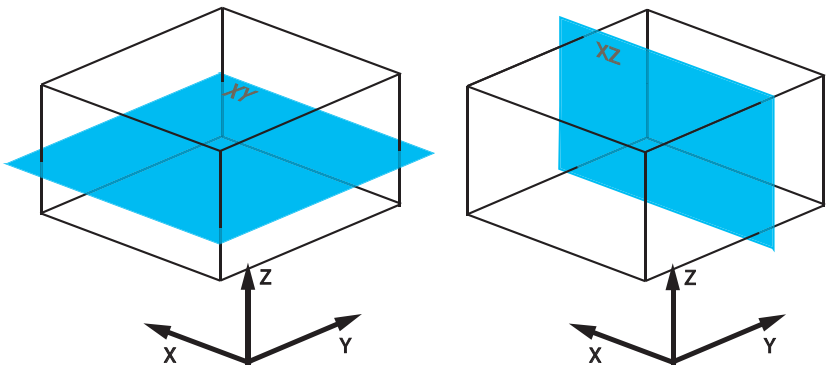

(a) Cutting plane for creating X,Y-plane (b) Cutting plane for creating X,Z-plane

Fig. 10 Cutting planes for creating cross sections of cubic parts (Z-axis is building direction)

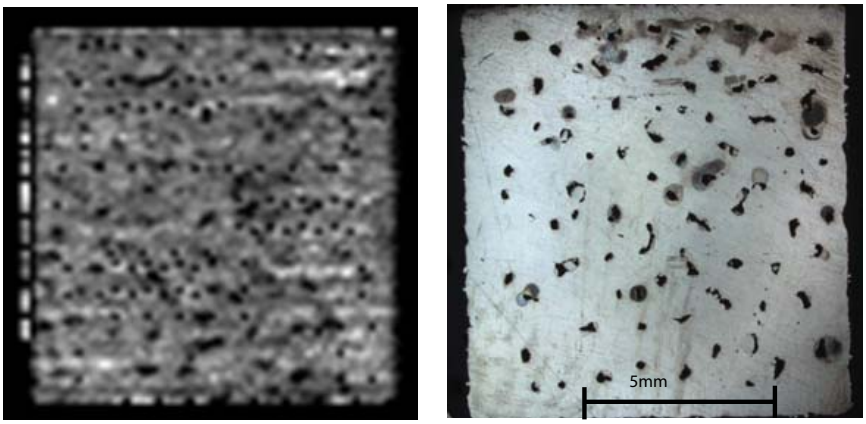

(a) Mapping of the X,Y-plane (b) Microscope image of a X,Y-plane

Fig. 11 Comparison of the mappings and the microscope image of a X,Y-plane

3.4 Detection of Pores Positions in three dimensions

To ensure the quality of a full part, all data monitored throughout an entire job can be bundled and analyzed together. As shown in previous sections the mappings of a plane can be linked to the porosity in that plane. By stacking the layer mappings on eachother, a 3D voxel model can be generated. This model indicates the quality throughout a full job. This method is very similar to the CT or MRI methods

used in medical imaging. By using standard thresholding methods (similar to the confidence intervals) it is possible to detect porosities.

By using medical imaging software such as Mimics, cross sections in any direction can be made. An example of such cross section in the X,Z-plane is illustrated in figure 12(a). This image is a cross section of all the stacked mappings of the layers. As seen, the porosities in figure 11 are regularly formed. The low sensor values of the melt pool always seems to occur on the same X,Y-position throughout the layers. To validate the in-situ result, the part was cut parallel to the building direction (figure 10(b)) and again the pores were clearly visible (figure 12). These figures show an excellent compatibility between the real microscope images and in-situ mappings. It should be noted that the thresholding algorithm and the confidence intervals of AlSi10Mg still requires further modification by using more empirical data to improve the accuracy. However it is important to notice that pores in the microscopic image are not located on the same locations as on the mappings. The mismatch between the similar X,Z- or X,Y-planes for mapping and microscopic images is due to the polishing of the specimen. Polishing exactly in a known plane is impossible. Both images show similar trends vertical pores in the X,Z-plane and a pore pattern in the X,Y-plane and are expected to match. To validate this some further tests have been conducted to validate the mappings with Computed Tomography.

3.5 Validation

Since it is rather impossible to create microscopic images in a plane that can be reconstructed in the mappings, a different approach to validate the correlation

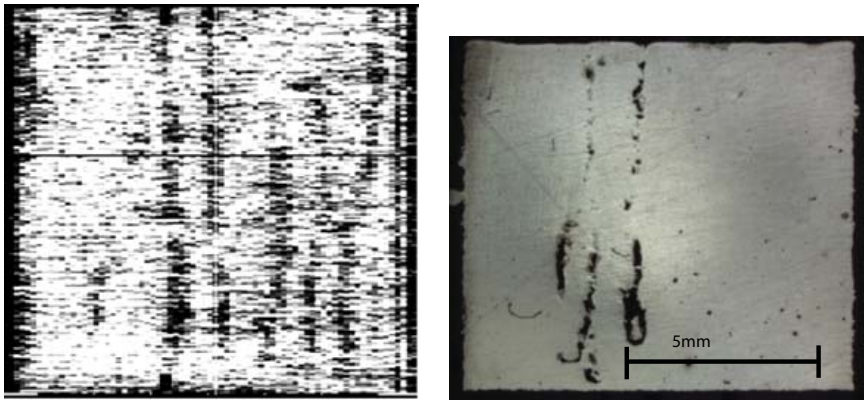

(a) Mapping of the X,Z-plane (b) Microscope image of the X,Z-plane

Fig. 12 Comparison of the mappings and the microscope image of a X,Z-plane

between mappings and pores was tested. This strategy compares the generated mappings with X-ray Computed Tomography. The material used for this validation is NiTinol and AlSi10Mg. By using a reconstructed 3D model from the mappings and from the CT measurements, both sample models can be examined on the same location.

Figure 13 shows an example of a cross section in the X,Y-plane of the mappings and the CT model for NiTinol. It is clear that the pore seen in the CT model is induced by the melt pool variation on the mapping image. This indicates that the monitoring system is able to detect defects.

To validate the robustness of the system for different materials, a validation test is also conducted on AlSi10Mg. The correlation between the mappings and pores is visible during the production of a mould with cooling channels (figure 14). Relative big pores marked with a highlighted circle (by a thresholding algorithm) in the CT image can be traced back on the mappings, which show on the same locations a rather dark spot due to melt pool variations. Despite the correlation

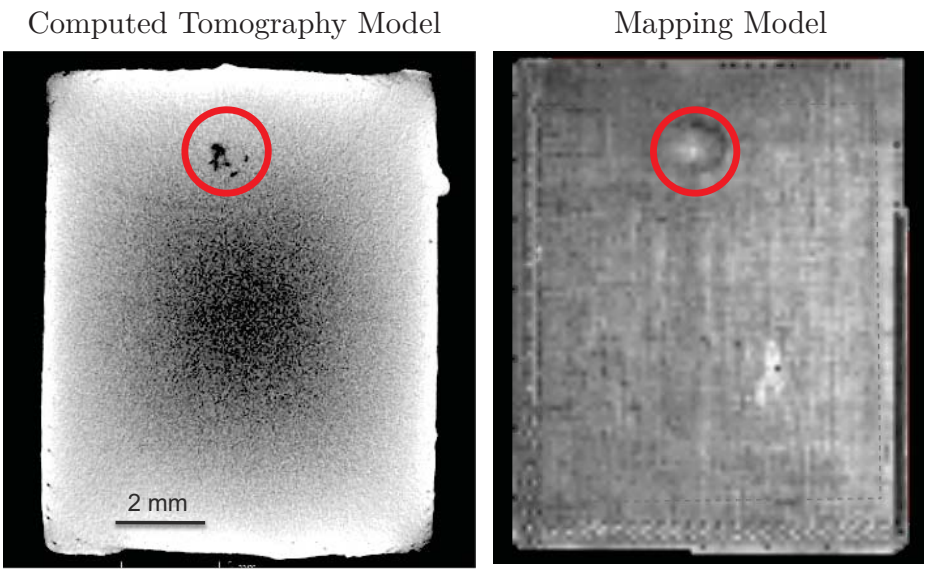

Fig. 13 Comparison of mapping model and X-ray CT model, NiTinol

also other melt pool variations are visible on the mappings which do not induce any defects visible on the CT image. Therefore further research needs to be conducted for filtering out irrelevant melt pool variations. By comparing these two models it shows that the monitoring system can be used to detect pores in SLM produced samples. However some more filtering should be developed to enable automatic error detection of a part.

The resolution and accuracy of this quality control system is determined by the mapping algorithm and the sample rate. Currently each pixel of a mapped image is $100\mu m$ by $100\mu m$. The pixel size is selected based on the expected melt pool size (around 120-$150\mu m$ diameter) and sample rate. Therefore a pixel where the melt pool is mapped will definitely be influenced by the measured melt pool signal. The automatic detection of very small pores (smaller than $100\mu m$) will need, due to the big pixel size, a more complex algorithm than just tresholding.

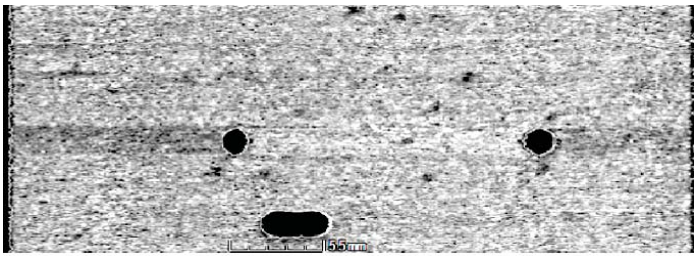

(a) Mapping of the X,Z-plane (AlSi10Mg)

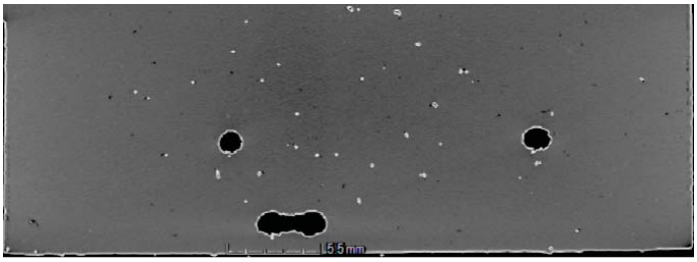

(b) CT crossection image of the X,Z-plane (AlSi10Mg)

Fig. 14 Comparison of the mappings and X-ray CT model (the three big holes are cooling channels) , AlSi10Mg

4 Conclusions

In this work, the in-situ monitoring system on the SLM machine is explained in detail. The set-up consists of a photodiode and a near-infrared thermal CMOS camera together with the data capturing and processing system. This dedicated implementation tool is essential to reach the high requirements for monitoring and logging of melt pool data of the SLM process at high sample rates. This set-up enables the operator of the SLM process to log melt pool intensity, area, length and width, at a sample rate of at least 10kHz and up to 20kHz. These sensor values are even available in real-time to make feedback control possible in the near future.

Afterwards the data processing and interpretation of sensor values are extensively discussed. Vectors are classified into different zones of different heat flow situation and/or different parameter sets. For each of these classes, a confidence interval is defined, which assists the interpretation process of the signals. Once confidence intervals are defined for the different classes, errors can be detected in parts produced by SLM.

The reliability of the in-situ quality control was examined using experimental data after manufacturing parts. The results on Ti6Al4V, AlSi10Mg and NiTinol parts show an excellent compatibility between the actual defects (revealed after cutting the samples or scanning them with X-ray CT) and what is observed from in-situ quality control. Accordingly, the described monitoring system can be successfully employed to reveal the quality of a part during and after manufacturing. It should be noted that the research is still ongoing to enhance the detection resolution of defects such as porosity.

5 Future work

In this work, the principle of the monitoring system is proven to be successful. However, further empirical data (obtained from various materials and manufacturing parameters) is required to extend the confidence intervals for different classes of materials and to improve the robustness of the system. Afterwards, basic algorithms like thresholding together with some filters can be used to automatically detect errors and/or process failures.

Acknowledgements The authors would like to thank Concept Laser GmbH, for the interesting collaboration, discussions and support in this field. Part of the research has received

funding from the European Union's Seventh Framework Program (FP7/2007-2013) under grant agreement number 314055.

References

1. Abe, F., Osakada, K., Shiomi, M., Uematsu, K., Matsumoto, M.: The manufacturing of hard tools from metallic powders by selective laser melting. Journal of Materials Processing Technology **111**(1-3), 210 – 213 (2001). DOI 10.1016/S0924-0136(01)00522-2
2. Berger, U.: Rapid tooling and computertomography for aluminium casting of automotive components. In: uRapid 2001 International users conference on rapid prototyping & rapid tooling & rapid manufacturing (2001)
3. Bourell, D.L., Leu, M.C., Rosen, D.W.: Roadmap for Additive Manufacturing: Identifying the Future of Freeform Processing. The University of Texas at Austin, Laboratory for Freeform Fabrication, Advanced Manufacturing Center (2009)
4. Chivel, Y., Smurov, I.: On-line temperature monitoring in selective laser sintering/melting. Physics Procedia **5, Part B**, 515 – 521 (2010). DOI 10.1016/j.phpro.2010.08.079
5. Clijsters, S., Craeghs, T., Kruth, J.P.: A priori process parameter adjustment for SLM process optimization. In: VRAP Int. Conf. Advanced Research in Virtual and Rapid Prototyping, pp. 553–560. Leira (2011)
6. Clijsters, S., Craeghs, T., Moesen, M., Kruth, J.P.: Optimization of thin wall structures in selective laser melting. In: Direc Digital Manufacturing Conference. Fraunhofer, Berlin (2012)
7. Craeghs, T.: A monitoring system for on-line control of selective laser melting. Ph.D. thesis, KU Leuven (2012)
8. Doubenskaia, M., Pavlov, M., Chivel, Y.: Optical system for on-line monitoring and temperature control in selective laser melting technology. Key Engineering Materials **Volume 437**, 458–461 (2010)
9. Kempen, K., Thijs, L., Humbeeck, J.V., Kruth, J.P.: Mechanical properties of alsi10mg produced by selective laser melting. Physics Procedia **39**, 439–446 (2012)

10. Klocke, F., Wirtz, H., Meiners, W.: Direct manufacturing of metal prototypes and prototype tools. In: Proceedings solid freeform fabrication symposium, Austin, august 1996 (1996)
11. Kruth, J., Van Vaerenbergh, J., Mercelis, P., Lauwers, B., Naert, I.: Dental prostheses by selective laser sintering. In: 10mes Assises Europennes de Prototypage Rapide, Paris, 14 & 15 September 2004 (2004)
12. Kruth, J.P., Deckers, J., Yasa, E.: Experimental investigation of laser surface remelting for the improvement of selective laser melting process. In: SFF 2008 (2008)
13. Kruth, J.P., Mercelis, P., Vaerenbergh, J.V., Froyen, L., Rombouts, M.: Binding mechanisms in selective laser sintering and melting. Rapid Prototyping Journal **Vol. 11/1, pages 26-36** (2005)
14. Lott, P., Schleifenbaum, H., Meiners, W., Wissenbach, K., Hinke, C., Bültmann, J.: Design of an optical system for the in situ process monitoring of selective laser melting (SLM). Physics Procedia **12, Part A**, 683 – 690 (2011). DOI 10.1016/j.phpro.2011.03.085
15. Rangaswamy, P., Griffith, M., Prime, M., Holden, T., Rogge, R., Edwards, J., Sebring, R.: Residual stresses in LENS components using neutron diffraction and contour method. Materials Science and Engineering: A **399**, 72 – 83 (2005). DOI 10.1016/j.msea.2005.02.019
16. Rehme, O., Emmelmann, C.: Rapid manufacturing of lattice structures with selective laser melting. Proceedings SPIE Photonics West, LASE, 2006 Symposium (2006)
17. Shiomi, M., Osakada, K., Nakamura, K., Yamashita, T., Abe, F.: Residual stress within metallic model made by selective laser melting process. CIRP Annals - Manufacturing Technology **53**(1), 195 – 198 (2004). DOI 10.1016/S0007-8506(07)60677-5
18. Thijs, L., Verhaeghe, F., Craeghs, T., Humbeeck, J.V., Kruth, J.P.: A study of the microstructural evolution during selective laser melting of Ti-6Al-4V. Acta Materialia **58**(9), 3303 – 3312 (2010). DOI 10.1016/j.actamat.2010.02.004
19. Voet, A., Dehaes, J., Mingneau, J., Kruth, J.P., Vaerenbergh, J.V.: Study of the wear behaviour of conventional and rapid tooling mould materials. In: International Conference Polymers & Moulds Innovations PMI, Gent, Belgium, April 20-23, 2005 (2005)

Click here to download Supplementary Material: IJBib.bib